ADDIS ABABA INSTITUTE OF TECHNOLOGY
SCHOOL OF CIVIL AND ENVIRONMENTAL ENGINEERING

3D Gravity Inversion for Mineral Exploration over Southern Green Stone Belt of Ethiopia

A Thesis Submitted to School of Civil and Environmental Engineering in Partial Fulfillment of the Requirements for the Degree of Master of Science in Geomatics and Geodesy

By: Girum Ashenafi

Advisor: Dr. Tulu Besha

March 18, 2022
Addis Ababa, Ethiopia

Approval sheet

The undersigned certify that they have examined the final thesis entitled with "**3D Gravity inversion for mineral exploration over southern green-stone-belts of Ethiopia**" and it is the original work of Girum Ashenafi carried out under the supervision of Dr. Tulu Besha.

Approved by the board of examiners:

Dr. Tulu Besha (Advisor)	_____ Signature	_____ Date
Sintayehu Abie (Internal examiner)	_____ Signature	_____ Date
Dr. Walyeldeen Godah (External examiner)	_____ Signature	_____ Date
_____ (Chairperson)	_____ Signature	_____ Date

Declaration

This is to declare that the thesis presented here is prepared by **Girum Ashenafi**, entitled with "**3D gravity inversion for mineral exploration over southern green stone belts of Ethiopia**" and all material used in the project have been acknowledged properly

Girum Ashenafi	_____	_____
Name of candidate	Signature	Date

Abstract

Mainly this study aimed to investigate subsurface geology of the southern green stone mineralization zone for evaluation of gravity inversion is how effectively detecting high-density mineralization. Throughout the project, three main tasks have done: the first task was carrying out necessary correction for observed gravity data. Under this stage three main outputs were obtained: Bouguer gravity anomaly, regional Bouguer anomaly and residual Bouguer anomaly. The target information is represented by residual anomaly therefore it is became the final data for inversion process. The second task was minimizing Tikhonov's cost function and carrying out inversion with the help of a conjugate gradient algorithm after formulated sensitivity matrix. The interpretation process was the last step of the work. The results obtained from the inversion process are demonstrated in two forms: the first one was a horizontal slice that illustrated the trend of mineralization in a horizontal plane and the second was density contrast model in a vertical plane that illustrated at four different lines of cross-section. In the horizontal density contrast model, the pixels value of high-density contrast under mineralization zone revealed 76.8% of pixels made a good agreement with the mineralization history of the target region. In addition, 90.3% of high-density contrast agreed with the location of metallic minerals in the region. In contrast, very low-density contrast in the region scored 3.77%. Therefore the inverted density contrast model well demonstrated the signature of mineralization in the target region. The vertical slice of the density contrast model indicated the depth condition of the high anomalous density region. Thus cross-section profile 1 up to 4 maximum depth and percentage of high density contrast above 600m depth are 1309.464m, 1089.866m, 847.72m, 661.0338m and 81.5%, 72%, 86.3%, 99.1% respectively. The vertical patterns of high-density contrast are correlated with the information obtained from a borehole at the mineralization zone. From such results and validation, I concluded: gravity anomaly inversion is a good tool to detect the position, depth extent, and the trend of the significant anomalous region.

Keywords: Inversion, gravity anomaly, Tikhonov regularization, density contrast

Acknowledgments

I would like to thank my advisor Dr. Tulu Besha for his academic advice and guidance during the progress of this study. His great academic support and advice were helped me to the successful accomplishment of this study.

I would like to thank Dr. Andinet Ashagre for his great academic advice, encouragement, and facilitating necessary material during the progress of this study. In addition, I would like to admire his wonderful and kind willingness to offer endless support throughout the progress of this study.

I would like to thanks Dire Dawa University for award this opportunity to follow up Msc program

I would like to thank the institute of a geological survey staff member for their kind helps to facilitate necessary geological information.

Finally, I would like to thank all my friends, Abiy Tamrat, Sadik Showmollo, Samueal Milki and to all my family for their scientific advice, discussion, and encouragement as well as for all other assistance during the progress of this thesis work.

Table of content

List of Figures

List of Tables

List of Acronyms

ANN	Artificial Neural Network
BC	Bouguer Correction
CBA	Complete Bouguer Correction
CS	Cross-Section
DC	Direct Current
DNSC	Danish National Space Center
GALILEO	European navigation satellite system
GCV	Generalized Cross Validation
GLONASS	Global Navigation Satellite System
GPS	Global Position System
GRS	Geodetic Reference System
GSE	Geological Survey of Ethiopia
IGSE	Institute of Geological survey of Ethiopia
Mgal	Mill gal
MS	Micro Soft
MSL	Mean Sea Level
N-S	North-South
QGIS	Quantum Geographical Information System
TC	Terrain Correction
3D	Three Dimension

Chapter One

1. Introduction

1.1 Background of the Study

The gravity measurement is one of the important tools for the investigation of subsurface geological information which are used for various real-world applications. The development of high accuracy instrumentation and stable observation platform since 1980 G.C has made large scale air borne gravity survey become possible and it could provide a chance to carry out broad extent projects that related to geodetic and geophysical work (Cai et al., 2018). The gravitational acceleration obtained from the measurement depicts the attraction power of masses that resides in the subsurface geology of the earth. This relationship of gravitational acceleration observed at the specific location and underlying mass distribution are firstly formulated by famous English mathematician sir Isaac Newton. The concept of this mathematical formulation is defined as the magnitude of the force between two masses is equal to the multiplication of the magnitude of individual mass and the inverse distance square between two masses. This is the very beginning mathematical formulation for the gravity-mass relationship. But when we bring such a concept to the geophysical problem, well-known integral representations of gravity anomaly equations have been used as a key mathematical formulation for revealing gravity anomaly due to geological anomalous mass.

Recently gravity inversion has become an essential tool for a vast geophysical investigation throughout the world especially in the sector of mineral exploration it has brought voluble outcomes. The inherent relationship of gravity and causative mass distribution are easily justifying the effectiveness of the gravity method for oil exploration and mineral prospects. Numerous previous researchers have been demonstrated the suitability of gravity inversion i,e which types of anomalous mass of geology can be recovered efficiently (Mandal et al., 2015; Essa & Munschy., 2019; Cai et al., 2018). For instance, salt dome detection, oil exploration, mineral prospect and to estimate the depth of sedimentary basin as well as to detection subsea basalt which is usually associated with the oil reservoirs are the geological anomalous object that has been recovered by gravity inversion of the corresponding region (Cai et al., 2018).

The main important parameters that can obtain from gravity field are the trend, size and depth condition of geological anomalous masses and their relationships of mineral resource occurrences. The basic information that directly inferred from gravity field is density distribution of underlying geology in target region. That means relatively higher gravity anomaly shows higher density or surplus mass in the vicinity. Conversely, the lower gravity field shows the lower average density (Chen, et al., 2018). Therefore density value is the basic parameter while we deal with gravity inversion for mineral exploration in a particular region of interest. Gravity inversion has been a technique of obtaining anomalous density distribution from a response gravity anomaly. To obtain required information (reasonable density) from inversion of gravity data, it needs to understand the appropriateness of techniques. Standard linear approach is the first one, under this approach the main assumptions is fixing the geometry of model cell then compute the unknown parameter which is called density contrast of model element. Such methodology has been used as the efficient algorithm to recover reasonable output that can show mineral resource with expected level of confidence (Vatankhah et al., 2019).

The second one is nonlinear gravity inversion which is usually used to determine the depth to the basement or the geometry of the sedimentary basin and for hydrocarbon exploration. In addition to these techniques, other many specialized techniques have been designed and used for ensemble reasonable subsurface geology for instance graph theory approach for 3D inversion of gravity data in which the subsurface body is modeled as an ensemble of point masses (Vatankhah et al., 2019). These and other several kinds of inversion techniques have been deployed in different previous works depending on its suitability for target investigation conditions and its capacities to incorporate prior knowledge or constraint.

The ill-posedness of gravity inversion has always been affected by the problems which are non-uniqueness and instability of the solution to be recovered. While the inversion process has been carried out, such kind of problem is usually common due to the number of observed data being much smaller than the number of model parameters. This sort of condition is said to be under determined problem i,e so many models or solutions may bring observed data (nonuniqueness) and small perturbation in model space are bring a large perturbation in data space called instability (Gupta, 2011). Therefore to treat such kind of problem most previous researchers have always used a mathematical optimization technique that helps to treat nonuniqueness and

instability problems. The basic task of this algorithm is to introduce an appropriate objective function that contains two parts, the first one is the misfit function for least-squares fitting of observed data and the second is the model objective function as a stabilizer for regularizing subsurface density distribution (Liang et al., 2014). Another consideration that should be involved while we introduce objective function is the ability to incorporate various prior information and constraint. Hence the formulation of flexible objective function finalized the next operation is executed minimization process to obtain single optimum density model of the region. Another requirement that needs to involve under the regularization process is a selection of optimum regularization parameters that helps to keep the tradeoff between solution norm and residual norm (Liang et al., 2014). The algorithm that used to calculate optimal regularization is called L-curve criterion. Under this algorithm the assumption is plotting the curve between solution norm and residual norm in vertical and horizontal axis respectively, then the regularization parameter that lies at or nearby the corner of L-shaped curve is selected as optimum regularization parameter (Gupta, 2011).

The overall target of the study is to interpreter the recovered density distribution of the region. The process of interpretation is based on the correlation between recovered approximate physical properties and corresponding rock properties and the mineralization nature of the respective rock in the region of interest. The final result will delineate the abundant anomalous mass distribution of subsurface geology that is related to the occurrence of mineral in the region of the study. Specifically, the occurrence of mineral deposits is inferred from the approximate density contrast of each model cell with the corresponding rock's physical properties and its mineralization nature.

1.2 Statement of the Problem

Mineral exploration histories in Ethiopia have gone for the past four decades since the foundation of the Geological Survey of Ethiopia in 1968 G.C. After the foundation of GSE and later reformed as Institute of Geological Survey of Ethiopia (IGSE) has done various work for investigation of mineral deposit and other related issues of the region. The scope of the tasks has generally been covered from the mapping of the geology up to drilling operation at a different particular area in the region of interest that helps to detect and document information about the mineral resource. According to the documentation of IGSE, various progress has been carried

out in the sector of the mineral resource by a few foreign and domestic companies with cooperation to the minister of mineral and energy resources of Ethiopia. In addition to this various interested academic and other researchers have tried for further investigation to improve the capacity of deep insight toward subsurface mineral resources of the region. Since geology is inherently complicated and the resource is concealed under the ground surface, the endeavors described above are not sufficient to obtain enough information about the mineral potential of the region. Rather it requires further detailed investigation using different kind of sophisticated techniques that helps to reveal an undiscovered section of mineral deposit in the region. As far as the mineral resource is the main source of significant revenue and has a key role in the development of one's country, it needs to adopt further investigation techniques and exploration capacities in an aspect of utilizing advanced technology and novel algorithms. Recently various researches have been done across the world that can demonstrate the efficiency of gravity inversion to mineral exploration and can realize the method from small scale up to large scale area. Therefore this study interested to combine gravity inversion with incorporating geological information as a constraint to obtain a plausible result of underlying density. In addition, the method can provide a good opportunity to look in deep and shallow anomalous masses of complex subsurface geology with respective geometry and depth as well as to provide further information for the future researcher that will use for further studies. In general, this study going to determine the approximate density distribution of subsurface geology and interpret the result density contrast using correlation of surrounding rock physical properties and mineralization nature of the rock in the region.

1.3. Objective of the Study

1.3.1 General Objective

The general aim of this study is 3D modeling of subsurface geology for the application of metallic mineral exploration based on the correlation of density to be recovered from inversion of gravity anomaly and known geological information.

1.3.2 Specific Objective

To attain the expected general aim of the study the following specific objectives are required to accomplished throughout the process.

- Estimating the approximate density contrast of model cells in a horizontal and vertical direction of the target region
- Formulating appropriate functions and constraints to the inversion process
- Evaluate the accuracy of recovered density contrast distribution of subsurface geology
- Interpretation of the recovered density distribution from corresponding geological information to analyze the mineralization nature of the subsurface geology

1.4 Research Questions

The research questions that are answered at the end of this study are focused on the following basic questions that help to investigate the problem.

- How effective is gravity inversion to show a clear trends and geometry of density anomaly?
- Does the gravity inversion technique bring a reasonable density contrast image of the subsurface?

1.5 Significance of the Study

The study mainly focused on carryout gravity inversion for a selected area of interest. The basic aim of the study is to apply the gravity inversion technique for the selected mineralization zone and then justify the effectiveness of the algorithm. This is mainly required because of the following reason. Firstly, geology has a nature of inherently complicated and concealed below the ground surface such condition makes the sector of mineral exploration always active to develop and test further algorithm that helps to improve the capacity of exploration. On the other hand mineral resources have a big role in world wide market so that it can bring significant revenue for one country. Therefore it is appropriate and reasonable to test and develop a further algorithm that helps to bring valuable outcomes for the sector of mineral resources.

In general, this study is interested to apply the gravity anomaly inversion technique for the selected region of interest. Throughout the study, various specific parameters, prior geological information, gravity correction, and other appropriate functions are applied. All available information is applied that helps to recover a clear image of mineralization. In the end based on the information incorporated in the inversion and recovered result the degree of effectiveness of gravity inversion is justified.

Ultimately the study provides the necessary recommendation to use gravity inversion for mineral exploration with a degree of effectiveness and appropriate condition that helps to recover plausible results. In addition, the study plays a role in providing a piece of possible information and knowledge for future researchers who works for the common good of the country and the development of the novel algorithm.

1.6 Thesis Outline

The current study is organized into five chapters that consist necessary description of the study. The flow of each chapter is based on the coherence of the idea starts with the introduction then proceeding with theory, method, expected output, and finally end with the conclusion and recommendation.

Chapter one is the introductory section of the paper. This chapter presents the following important components of the paper: background of the study, the objective of the study, statement of the problem, research questions.

Chapter two presents the theoretical background knowledge about various algorithms related to gravity, inverse problem, and the review of previous work carried out around the world and local situations.

Chapter three presents three basic issues: the first section is a description of the study area and the data types used, the second section is a description of data preparation and correction that tends to be input parameters to inversion and the third section of this chapter involves the main part that describes the detail procedures and method that are used for inversion process.

Chapter four presents the result or the output of the study in the form of an image and text description. In general, this chapter involves the demonstration of density contrast in a vertical and horizontal plane for the target area.

The last chapter in the content of this paper is chapter five that presents the conclusions of the study that are inferred from the entire process of the work and the recommendation.

Chapter Two

2. Literature Review

2.1 Basic Theory of Gravity

The fundamentals of gravity theory began long years ago. The famous English mathematician Sir Isac Newton had discovered the gravitational acceleration principle and related mathematical formulation for the first time. The mathematical formulation of this law is defined as the attraction force between two bodies is directly proportional to the individual mass and inversely proportional to the square of the distance between them. Another one that is concerned about the acceleration of a body is Newton's second law of motion, which states that anybody of mass (m) under the effect of force (f) moves with the acceleration (a) (Alsadi and Bahan, 2014). By combining these two laws, for the two mass systems, the following relationship is readily obtained.

$$a = G\frac{m}{r^2} \qquad (2.1)$$

On the other hand, when dealing with a particle mass $\triangle m$ would create acceleration $\triangle g$ at an observation point at r distance away is given by

$$\triangle g = G\frac{\triangle m}{r^2} \qquad (2.2)$$

This mathematical formulation is the general principle that helps as starting concept for further investigation about the potential field-related issue. Generally, our interest is conceptualizing the relationship between potential fields and causative bodies based on the mathematical equation. The potential field is the scalar field that emanates from the source masses which are occupied with different elementary masses. Due to such field the body in the vicinity experiences attraction force. Thus force per unit mass is acceleration which has a similar magnitude as equation 2.1. The acceleration caused by gravitational potential of the earth is known as acceleration due to gravity. Two basic reasons are makes gravity vary at all point the earth. Thus are: the earth is not perfect sphere due to rotation and internal mass redistribution.

Gravitational potential field most usefully defined in terms of U:

$$U = \frac{GM}{r} \quad (2.3)$$

Gravitational potential is the scalar quantities (represented by magnitude) that can show the attraction potential due to the naturally existing mass (Kearey et al., 2002). In global context such potential of the earth has often been modeled in the forms of spherical harmonic expansion. The underlying mass distributions in the vicinity of gravity observation plane are the cause for gravity variation in the region. From gravitational potential, it is possible to derive the gravitational acceleration. That means the differentiation of gravitational potential in a particular direction provides the gravity component in that direction so that gravitational acceleration is vector quantities described by both magnitude and direction. Such kind of fact makes gravitational potential being computational flexible (Kearey et al., 2002). Gravitational potential can be used for various applications but the main and basic application in geodetic science has been to establish a reference surface for height measurement known as the geoid. This surface is represented by a constant gravitational potential surface mostly known as equipotential surface.

Generally, this potential is naturally existing potential that helps to determine the shape, volume, and size of the earth as well as to detect various phenomena that happen due to the dynamic nature of the earth. To model such events, a technologically advanced instrument is required to measure gravitational potential with high accuracy. Recently various gravity surveying techniques has been deployed to measure with sufficient accuracy which helps to enhance the capacity of insight toward target information which is dedicated to the required real-world practical applications. In the following topic, the principle of gravity measurement and various measurement techniques will be described briefly to provide the background concept behind measuring instruments.

2.2 Measurement Principle of Gravity

The gravity measurement device is known as a gravity meter or gravimeter, this instrument has commonly used to measure the gravitational acceleration of the earth. Mainly while we measure gravity, the stability of the measuring device is another thing that should be considered. Different kind of platform has been deployed to mount the gravimeter on it to obtain stable instrumentation those are space-based (satellite gravimeter), airborne (aircraft), and terrestrial gravimeter. Firstly we are going to discuss the principle of gravimeter used to measure the

gravitational acceleration as the response for underlying mass change and then later a brief description about the platform.

Gravimeter

A gravimeter is a device used to measure the gravitational acceleration induced by underlying mass distribution at a particular region of interest. Mainly this device used basic physics principle which is called Hook's law. The device is mounted with the spring and constant mass with appropriate geometry it varies with the types of gravimeter. The fundamental working principle of the gravimeter is based on mass-spring system of Hook's law. The constant mass hangs on the spring in the system of gravimeter is attracted by other mass in the vicinity outside the device system. The degree of attraction force depends on the external mass that influences the closed spring system of the gravimeter. When the device is nearby excess mass, the constant mass attached with the spring in the device is attracted with high magnitude toward the excess mass relative to the surrounding so that the spring is more stretched. In contrast when the external mass in the vicinity of the device is less relative to the surrounding, then the magnitude of attraction is less as a result the stretching length of the spring becomes less. In general, such a system is clearly described by Hook's law, which states that the extension of the spring is proportional to the force (Jones, 2007). Mathematically described as:

$$F=ks \qquad \& \qquad F=ma$$

$$mdg = kds \qquad => \quad dg = ds\, k/m \tag{2.4}$$

Where k is elastic spring constant, ds is a small change in length of spring because of a small change in gravitational acceleration. In general, the magnitude of measurable gravity anomaly in geophysics is in the range of 0.1 to 0.00001 gal this implies the condition that we must measure the gravity of 1 part in 10^8 (Jones, 2007).

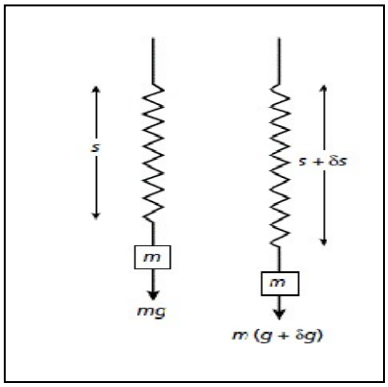

Figure 2.1 *Principle of stable gravimeter operation (Kearey et al., 2002)*

Various types of gravimeters have been produced throughout the time from early up to advanced modern one. The technological advancement and demand of high-level precise instrumentation for various geodetic applications enforced to invent more sophisticated devices throughout the time. Based on the difficulty in the measurement in the aspect of precision, sensitivity, and overall efficiency the latest device is more advanced than the early gravimeter. The sensitivity of early gravimeter has highly restricted because of the mechanism of the spring system. This means the spring system in a stable gravimeter has a dual function one is supporting the mass and the second is serving as a measuring device. Such a kind of defect leads the scientist to develop other gravimetric devices that can overcome the problem (Kearey et al., 2002). Such kind of modified gravimeter device is called an unstable gravimeter.

Commonly known unstable gravimeters are Lacoste & Romberg gravimeter, Worden-type gravimeter, and Bell gravimeter. Lacoste & Romberg gravimeter is unstable kind of gravimeter (Kearey et al., 2002). The spring system mounted in the device differs from static gravimeter. The arrangement and geometry of the spring system that is mounted in the device are arranged in a way to enable it to measure without the problem mentioned under the properties of a stable gravimeter. The basic component assembled in Lacoste & Romberg gravimeter is a hinged beam, carrying mass and spring that supports the hinged beam and mass. These components of gravimeter assembled in the form of revealed at Fig. 2.2. The basic working principle of this gravimeter is as follows: when the gravity increased because of nearby mass outside the device system, the beam is depressed as a result the extension of the spring increase. On other hand the restoring force of the spring increase, angle θ decrease to θ'. In general, the instrument is read by restoring the beam to horizontal by altering the vertical location of the spring attached with a

micrometer screw. The desired precision of gravity measurement depends on the design of spring & beam geometry. In Lacoste &Romberg gravimeter the thermal effect is removed by battery-powered thermostats (Kearey et al., 2002).

Another kind of unstable gravimeter is known as Worden-type gravimeter. The arrangement of the spring system in the device has similar mechanical arrangement but the difference is in the case of Worden-type the beam is supported by two springs, unlike the former one. The function of the first spring is to measure gravity while the second change level 2000 gu reading range of the instrument. In general, the overall reading range is similar to the Lacoste & Romberg. Another difference is Worden-type does not require thermostats rather thermal effect is removed by utilizing quartz component &bimetallic beam (Kearey et al., 2002).

Another kind of gravimeter that is the most successful axially symmetric instrument is known as the Bell gravimeter. Bell gravimeter is a more advanced and powerful device than the other described above. The components that built up the device differ from the previously described gravimeter. The sufficient accuracy & sensitivity of the Bell gravimeter is maintained by utilizing a magnetic and electric system. The accelerometer is used as a sensing element that is mounted on a stable platform within the system of the device. The system of the device worked when a DC passed through the coil causes the mass to act as a magnet and the weight of the mass balanced by a permanent magnet. In general, the sensor mounted within the device senses the change of the current due to vertical acceleration (Kearey et al., 2002). Ultimately gravimeters of all kinds aim to measure gravity change in the level of desired sensitivity and accuracy.

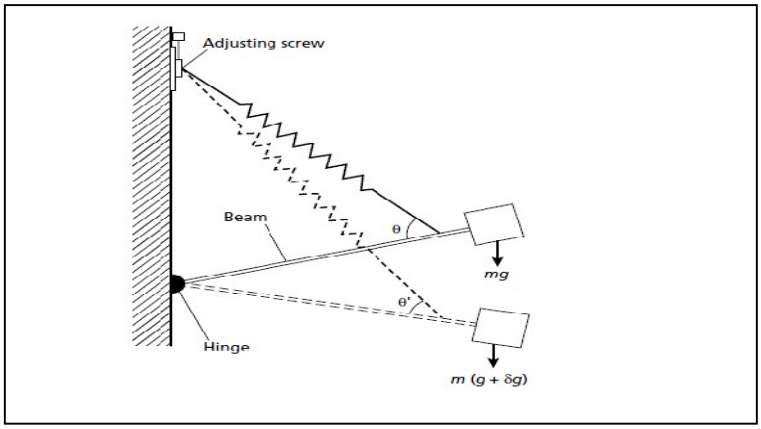

Figure 2.2 *Principle of the LaCoste and Romberg gravimeter (Kearey et al., 2002)*

Gravity surveying methods

Various kind of gravity surveying method has been employed for different application, thus are ground gravity surveying, airborne gravity surveying, marine gravity surveying, and satellite gravity surveying. These are commonly known gravity surveying techniques, each technique serves various applications based on its appropriateness for a particular purpose.

Terrestrial gravity measurement is the most common surveying method used for a long time in a geo-science application. The measurement system is based on a defined procedure and setup that helps to record all necessary information from field observation. At the field, the necessary information that is to be recorded are the location of the station (x, y, z), time of recorded, and gravity reading. Terrestrial gravity surveys are normally conducted in two general phases. The first phase is the establishment of a base station that helps to use as a reference station for other survey points. The second is surveying the preferred location and spacing that helps to get the desired level of precision for a specific application (Alsadi and Bahan, 2014). The main advantage of the terrestrial gravity survey technique is possible to measure with good accuracy because the measuring device (gravimeter) takes a record in stable condition this means the platform is stable nothing acceleration affects the gravimeter while it takes observation. But the disadvantage or difficulties in this technique is inaccessiblity of topography preclude taking observation in the form of evenly distributed. In addition, it is too costly and time-consuming to cover a large area of interest.

The second technique of gravity surveying is airborne in this case the measuring device is mounted on aircraft and the measurement is proceeding along the defined line of flight. While carryout measurement the flight altitude depends on the condition of underlying topography and atmospheric condition. Similarly, the accuracy of the data highly depends on these factors especially the atmospheric condition during measurement has a significant role to record in good precision. The main advantage of this technique is to acquire data that cover large areas simultaneously to observe local gravity variation. Airborne instruments have become capable of acquiring data with sufficient resolution to contribute towards resource-scale projects (Jones, 2007).

Another one is the marine gravity surveying technique the measurement of gravity carried out on the surface of the sea. The instrument is mounted on the moving ship so that the dynamic nature

of the sea surface affects the precision of measurement. But due to the oscillatory motion of the ship, the problem is easily fixed within a few minute by averaging (Kearey et al., 2002) . This technique is used for the various geodetic applications that are associated with the gravity on the sea surface and to study underlying conditions.

The last gravity surveying technique is satellite-based gravity observation. This technique mainly uses the satellite orbit to observe gravity variation due to mass anomaly. Two general concepts of gravity measurement based on satellite systems are satellite-to-satellite tracking (range and range-rate measurements between satellites), and satellite gravity gradiometry (measurement of gravity differences within the satellite).

Satellite-to-satellite tracking in the high-low mode*:* refers to low orbit satellite (a satellite dedicated to gravity field mission) is tracked by high orbiting satellites like GPS, GLONASS, or GALILEO (navigation satellite), relative to a network of ground stations. In this system, accelerometers are the important device that used to measure the effect of non-gravitational forces acting on the gravity field satellite. The low orbiting satellite is the gravity mission satellite that probe in the Earth's gravity field which can be precisely tracked without interruption. The observed 3-D accelerations correspond to gravity accelerations (Seeber, 2003).

Satellite-to-satellite tracking in the low-low mode: refers to gravity field satellites that are placed in the same low orbit, separated by several hundred kilometers, and that the range *D* between both spacecraft is measured by an inter-satellite link commonly it uses microwave with the highest possible accuracy (Seeber, 2003).

Satellite gravity gradiometer*:* this system works in the way that acceleration differences are measured directly in the satellite. Since the spacecraft is in free fall, the accelerations have to be measured away from the satellite's center of mass, ideally in all three dimensions (Seeber, 2003)

2.3 Gravity Correction

Because the earth is not a perfect homogenous sphere and the variation of internal mass distribution, the gravitational acceleration is not constant entire the surface of the earth. Therefore the magnitude of gravitational acceleration is different at every position on the earth. Mainly the magnitude of gravity depends on the following five factors: latitude, elevation, the

topography of the surrounding terrain, earth tides, and density variations in the subsurface (Valenta, 2015). Therefore correction must be carryout to those factors to obtain target anomalous gravity according to the information which we want to extract. The following section explains about necessary data correction that helps to extract target anomalous gravity due to anomalous density distribution.

Two general global factors cause gravity to vary with latitude; this means the earth flattening and its rotation about the polar axis causes the Earth's gravity to increase as the observation point moves from the equator towards either of the two poles (Alsadi and Bahan, 2014). Because of this reason, the gravitational acceleration measured at sea level uniformly increases with latitude from equator to pole. The approximate closed formula of normal gravity on the surface of the ellipsoid is given below as $\Upsilon(\varphi)$for GSR80 ellipsoid.

The latitude correction is achieved by subtracting normal gravity g(ϕ) from observed gravity value(g_{obs}) to obtain observed gravity anomaly $\triangle g_{obs}$.

$$\Upsilon(\varphi) = 9.780327 + 0.051630075\sin^2\varphi - 0.0002276\sin^4\varphi + 0.00000123\sin^6\varphi \quad (2.5)$$

$$\triangle g_{obs} = g_{obs} - \Upsilon(\varphi) \quad (2.6)$$

Because of elevation change, the corresponding gravity change is occurring. Change in gravity that occurs as a result of a change in elevation of the observation point is a function of thickness and density of the material found between the observation point and the datum level, which is normally taken at mean sea level. The corrections for elevation change are categorized into three classes thus are free air correction, Bouguer correction, and terrain correction (Alsadi and Bahan, 2014).

Free air correction means removing the effect of topography hence the materials between the observation point and mean sea level is air so that the name is called a free-air correction. Raising the gravity meter (e.g. extending its tripod) decreases the measured gravity values by 0.3086 mGal/m. to aquire gravity with the accuracy 0.01 mGal it is must to have elevation that are measured with the 3 cm accuracy (Valenta, 2015).

$$\Delta g_{FA} = g_{obs} - \Upsilon(\varphi) - 0.3086\left[\frac{mGal}{m}\right] * H \quad (2.7)$$

After correction, we obtain a free-air gravity anomaly. Bouguer correction carryout for removing the effect of rock density found between the observation point and mean sea level. Free air correction is only correct for elevation which does not account for the material density that lies between the observation point and reference datum (Alsadi and Bahan, 2014). The basic assumption in Bougeur correction is infinite horizontal rock slab with constant density 2670kg/m3 (the average density of crust) which has a constant thickness is used to remove the effect of a topographic slab that represented as Bouguer plate. Bouguer gravity correction is calculated by equation (2.8).

$$BC = 0.0419\rho H \text{ mgal} \quad (2.8)$$

Where BC is Bouguer correction in mill gal ρ is the density of surrounding topography(commonly 2670kg/m3 has been used in most cases), H is the thickness of slab or Bouguer plate. When we use the density value that we have specified before, the Bouguer correction is as the following.

$$BC=0.1119H\text{mgal/m} \quad (2.9)$$

Bouguer gravity anomaly is obtained after applying the correction on free air anomaly.

$$\Delta g_B = g_{obs} - \Upsilon(\varphi) + 0.3086H - 0.0419\rho H \quad (2.10)$$

In general, Bouguer's gravity values are negative over most of the continental areas and positive over oceans. In and around coastal regions, Bouguer gravity values are near zero-level (Alsadi and Bahan, 2014). This is a common worldwide observation.

After the correction has been made for the Bouguer plate it is necessary to assume that the correction to topographic irregularity i,e we have assumed a constant tick slab or plate while carryout Bouger correction but in reality topography is not as flat as our assumption made in Bouger correction. Therefore it requires some sort of correction for up hilling of terrain in surrounding of Bouger plate and for valley exist in surrounding of Bouguer plate. Elevated ground (such as hills) near an observation point creates a vertical component in gravity attraction reducing the gravity value at that point. Holes and valleys on the other hand represent a lack of material in parts of the assumed horizontal rock slab. In effect, these also create vertical components which would reduce the gravity value. Thus in normal situations, terrain correction

(TC) which is always positive is introduced to compensate for the topographic irregularities existing around the observation point (Alsadi and Bahan, 2014). The common method to calculate terrain correction is the hammer chart method has been used most of the time.

The complete Bouguer correction is obtained after applying terrain correction on a simple Bouguer anomaly then the final output is complete Bouguer anomaly. Thus:

$$\Delta g_B = g_{obs} - \Upsilon(\varphi) + 0.3086H - 0.0419\rho H + TC \quad (2.11)$$

Where: TC is terrain correction that is added to simple Bouguer anomaly.

2.4 Gravity Anomaly for Simple Geometrical Shape

Representation of subsurface of the earth in simple geometrical shape helps to effectively construct the response of anomalous bodies. As far as concerned about recovering subsurface structure from observed gravity anomaly. From the common definition of geological anomaly, any lateral change of subsurface geology of a given area is said to be a geological anomaly. This occurs as a result of a change in density of a horizontal layer or change in the horizontality of a constant-density layer (Alsadi and Bahan, 2014). These conditions contribute to occurring of anomalous gravity during the measurement of the gravity field. Therefore theoretical and mathematical formulations to such kinds of bodies are explained in this section of the paper. Numerous kinds of simple geometrical shapes have been used to approximate subsurface earth for computational simplification. Thus are: point mass approximation, spherical approximation, cylindrical approximation, horizontal thin slab approximation, and rectangular parallel piped approximation. Such simple geometrical approximated objects at a certain specific depth and in a different orientation as well as the behavior of gravity anomaly due to those objects are discussed in the following section of the paper.

From the geometrical approximation mentioned above, we can group them into rectangular and other geometrical approximations. The rectangular approximation is the most popular and good because it is being simple to numerical calculation and it is good enough to recover target space without gap plus in a regular fashion. Such kind of condition makes a rectangular approximation better than the other listed above. Other geometrical approximations have their advantage, particularly most of such approximations are used to model target specific body and to a body that can easily be approximated by those geometrical shapes. But for reconstructing the model

from a small simple body rectangular parallel piped is good and efficient. Therefore later section of the paper will discuss in forms of two categories rectangular and other simple geometrical approximation

2.4.1. Gravity Anomaly for other Geometrical Approximation

Under this section, four kinds of simple geometrical approximation and their mathematical formulation are clearly explained. In general, the main thing that illustrated here is the relationship of gravity anomaly due to simple geometry and the parameters that represent the body. Therefore all are discussed as follows.

Gravity anomaly of point mass means how gravity anomaly can behave for point mass which is buried at a certain specific depth (z). Point mass is the mass that all its mass is concentrated at its center and its dimension is like point. Therefore this section of the paper described the effect of a point mass on gravity measurement or in other words the response gravity anomaly for the point mass. The mathematical relationship for gravity anomaly due to point mass is described as follows. The vertical component of gravity effect (△g) of a point mass (△m), buried at depth (z) and distance (r) from an observation point (p) located on the surface (Alsadi and Bahan, 2014). Thus

$$\Delta g = \frac{G\Delta mz}{(x^2+z^2)^{\frac{3}{2}}} \tag{2.12}$$

Where G is the universal gravitational constant($6.67x10^{-11}m^3kg^{-1}s^{-1}$)

The second simple geometrical approximation described in the introduction section is spherical. The gravity anomaly of a solid sphere that is buried at a certain specific distance beneath the earth's surface has the following mathematical formulation. This geometrical shape is assumed as a geological anomaly that has a constant radius R and has density contrast p. And the equation (2.13) describes the gravity anomaly due to a solid spherical-shaped geological anomaly. Generally, this portion of the paper tries to demonstrate the effect of a solid spherical geometrical shaped object that is buried at a particular depth on the vertical component of gravity measured at the surface (Alsadi and Bahan, 2014).

The gravity anomaly (vertical component of gravity, Δg) of a buried sphere of mass (m), radius (r), and depth of its center-point (z) can be expressed as a function of x distance as follows

$$\Delta g = \frac{4\pi G p r^3 z}{3(x^2+z^2)^{\frac{3}{2}}} \quad (2.13)$$

The cylindrical shape is another type of geometrical shape that can be used to approximate subsurface geology to reduce the complicated nature of subsurface geological structure and to easily describe bulky subsurface geology into the elementary shape as a form of simple geometrical shape. The gravity anomaly due to a cylindrical-shaped object that is buried at a particular depth depends on the orientation of the object, this means the response of a horizontal oriented cylindrical object varies from that of a vertically oriented cylindrical object. In this section, a horizontally oriented cylindrical-shaped object (thin rod) is described for illustration purposes. Like the case of the sphere, a thin homogeneous cylinder can be approximated by a uniform line mass having the mass of the cylinder concentrated in its axial line. Applying this concept to an infinite horizontal cylindrical rod of the radius (d) and density (p), lying at depth (z). The gravity anomaly (△g) can be expressed as a profile along a line that extends in the direction of the x-axis which is taken as perpendicular to that of the cylinder's axis (Alsadi and Bahan, 2014)

$$\Delta g = \frac{2\pi p d^2 z}{(x^2+y^2)} \quad (2.14)$$

Another type of simple geometrical shape that helps to approximate subsurface geology is the horizontal thin slab shape. Like other approximations that we have seen above this kind of geometry is also possible to use for approximation of the subsurface of the earth but it depends on the target anomaly that we want to extract. The assumption behind this approximation is constructing subsurface geology from a horizontal thin slab that has a thickness of △z and lies at depth of z. And the horizontal thin slab is used as an elementary object that helps to ensemble the whole model space. The vertical component of gravity due to the horizontal thin slab which has a thickness (△z), density (p), depth at (z), and elementary volume of the strip (Alsadi and Bahan, 2014) p△z is given as follow:

$$\Delta g = \frac{2G\rho\Delta z\Delta xz}{(x^2+y^2)} \quad (2.15)$$

2.4.2. Gravity Anomaly of Rectangular Parallel- piped Shape

Rectangular parallel piped or rectangular prism approximation of subsurface geology is more suitable geometry than other simple geometrical shapes because the shape is suitable to reconstruct the whole model space from small rectangular prisms without any gap between edges of the blocks. The gravity effect of rectangular parallel piped can be computed by adding the contribution of each elementary rectangular prisms of rectangular parallel piped shape. The volume of the elementary shape (rectangular prism) is $\Delta x, \Delta y, \text{and} \Delta z$. The dimension of the elementary object is $\triangle x$ in the x-axis, $\triangle y$ in the y-axis, $\triangle z$ in the z-direction and the radial distance of elementary volume from observation point (p) is r (Alsadi and Bahan, 2014). The vertical component of the gravity at this point due to the elementary volume mass is given as follow:

$$\Delta g = G\frac{(\rho \Delta x \Delta y \Delta z)z}{(x^2+y^2+z^2)^{\frac{3}{2}}} \tag{2.16}$$

The gravity effect ($\triangle g$) for the parallelepiped at the point (p) is then obtained by successive definite integration over the dimensions of the parallelepiped. Thus

$$\Delta g = G\rho \iiint \frac{zdxdydz}{(x^2+y^2+z^2)^{\frac{3}{2}}} \tag{2.17}$$

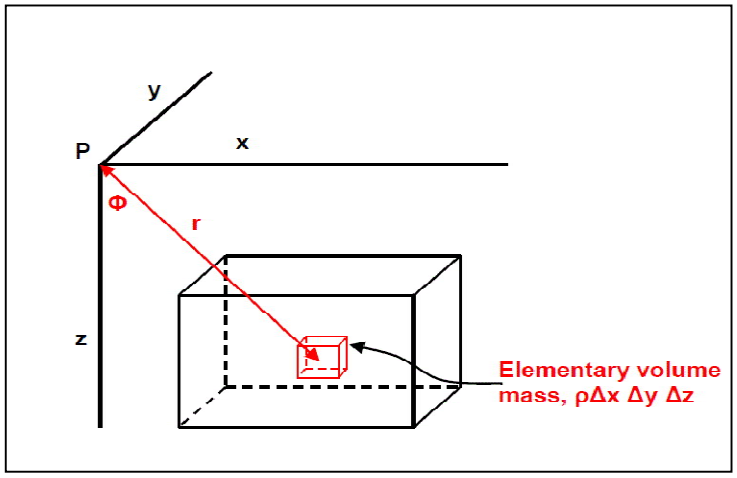

Figure 2.3 A rectangular parallelepiped with the elementary Volume mass (Alsadi and Bahan, 2014)

2.5. Inverse Theory

The inverse theory deals with the inverse transformation of forwarding operation; this means taking the inverse of forwarding operation matrix. Forward formulation or operation is the process of transform or mapping a function from pre-existing model space to data space mathematically, whereas inverse operation is mapping from observed data to model space by incorporating different apriori information and well-defined parameters. When we discuss real-world physical systems, there are lots of complicated situations that may arise which are not easily grasped or modeled. Such condition has been faced as a problem in the geophysical field of study. Because of target exploration or model space is being concealed under subsurface of the earth system. This underlying cause makes the process more complicated and leads many scientists to further investigation. Specifically, the main problem always faced in the inversion process is the system of the equation to be inverted may not have a solution or may have infinitely many solutions. Such kind of problem intends to investigate for a more mathematical or statistical approach to treat a problem that helps to control such a situation. In general, this section provides a detailed description of the inverse problem and related background principles.

When dealing with an inverse problem, the system of the equation is mostly fails to satisfy one of three Hadamard conditions that show the well-posedness of the system of equation (Gupta, 2011). Three Hadmard conditions that define a well-posed problem are as follow:

- ✓ The solution is exist
- ✓ The solution is unique
- ✓ The solution is stable

While solving inverse problems the system of the equation that fails to satisfy one of these conditions, then it is known as an ill-posed problem. In a general sense, inverse problems are inherently faced ill-posedness when the system of the equation contains much more model parameters than input data; in such case the system is called an underdetermined problem. Because of such conditions, the coefficient matrix of the equation that is formulated to carry out inversion is fails to satisfy the Hadamard condition. Hence such an underlying problem causes the solutions become complicated to get a unique and stable solution. Underdetermined condition of the inverse problem is the cause for the recoverable solution to be infinitely many; such problem is known as nonuniqueness. In other words, such kind of feature can be defined as

so many infinite solutions that are possible to reconstruct observed data. Another problem mostly faces while solving inverse problems is the instability of the solution. The small change in data space causes a large perturbation in the model so the nature of the solution becomes unstable. These two features of the ill-posed problem have been faced in inverse problems and make the process more complicated to obtain a reasonable solution from the inversion (Gupta, 2011).

Various previous works of gravity and other geophysical inversion face the above-described complication of an inverse problem. Because of the observation to be measured at limited discrete points cannot recover a large number of models. Therefore to overcome such problems optimizing or stabilizing the solution is a good mathematical treatment to control or reduce the instability of the solution. Generally, the discretizations of a linear inverse problem typically give rise to a linear system of the equation that is a very ill-conditioned matrix of ill-determined rank. To obtain a meaningful approximated solution for the linear system of equation, in general, requires that the system necessarily be replaced by a nearby system that is less sensitive to perturbation. This replacement is referred to as optimization.

The inverse problem has been solved using different mathematical or statistical operation that provides the best estimation about recovered parameters within a required uncertainty level. The most common algorithms that have been used in geophysical studies to solve an inverse problem are described in the following section.

Least square solution: Least square solution of a strictly over-determined problem was first proposed by Gauss in 1795 (Gupta, 2011). The least-square solution easily obtained even if system of equations has inconsistent nature. Here the solution is obtained by minimizing the residual norm.

$$\text{Minimize } e^Te = (b-Ax)^T(b-Ax) \tag{2.18}$$

$$\text{Solution } x= (A^TA)^{-1}A^Tb$$

Minimum norm solution: Minimum norm solution of a strictly underdetermined problem is obtained through constrained minimization of the L2 norms of the unknown vector x (Gupta, 2011).

$$\text{Minimize } x^Tx \quad \text{subject to} \quad b-Ax=0 \tag{2.19}$$

Solution $x = A^T (AAT)^{-1}b$

Artificial neural network: is an algorithm that is used to solve complex problems in many scientific studies for example for pattern recognition, classification, and generalization as well as in various geophysical investigations. The artificial neural network working principle is based on the way of functioning of biological neural network that means the input and output process organized in the form of a nerve cell or neuron interconnection and deals with how the massage transmission takes place in the specific cells structural and functional organization.

In general, the structure of a neuron is composed of three parts; the first one is the cell body or soma as the main body, the second is dendrites that are used to transmit a series of an input signals to soma. The third one is the axon used as a branch to transmit the output impulse (Sandham and Hamilton, 2011). Those branches or parts of a cell transmit a signal among a billion interconnected neurons. The detail of ANN is well demonstrated in the inverse theory, artificial neural network (Sandham and Hamilton, 2011).

The basics of algorithms' for geophysical studies are solving the linear system of equations by formulating the transformation matrix that can show the relationship between response vector y and target vector x.

- $Y= T[x]$ => forward modeling,
- $X=T^{-1}[y]$ => inverse modeling

To solve such a relationship especially the latter one the algorithm uses some procedure that contains a layer of input distribution nodes, number of hidden layers of perceptrons, and output layers (Sandham and Hamilton, 2011). These entities are interconnected and create new layers and the procedure continuo until to obtain the model that can well describe the data in a sufficient statistical explanation. The algorithm is complicated while implementing system to target the problem. This is to give a summary of the algorithm (Sandham and Hamilton, 2011).

Monte Carlo algorithm: This algorithm is another well-known method to solve an inverse problems based on the probabilistic approach. Mainly the algorithm lies on first random gauss or uses prior knowledge to the initial model then generates a new model by making a random perturbation to the current model (Sambridge and Gallagher, 2011). The new model was obtained after making perturbation known as the proposed model. Based on such a way the best

fit model is taken and other rejected this is determined by the acceptance criteria that describe at the later equation.

$$\alpha = \min\left\{1, \frac{p(m')p(d/m\prime)q(m/m\prime)}{p(m)p(d/m)q(m'/m)}\right\} \quad (2.20)$$

Where m and m' are proposed and current models respectively, q(a/b) is the probability of proposing model a, given a current model b and other distributions are as defined earlier (Sambridge and Gallagher, 2011).

Specifically, the decision depends on the parameter σ and random number u. this is done by comparing the value of σ with u, if u< σ the current model is replaced by the proposed model if not discard the proposed model and stay at the current model. Then such process continues for much iteration. Finally, the proposed model needs to be searched in the model space to achieve a reasonable balance between accepting and rejecting the proposed model. "The reasonable rate of acceptance is 30-40%". In general, the detailed procedure and steps of the algorithm are well described in inverse theory, Monte Carlo (Sambridge and Gallagher, 2011).

Genetic algorithm: Another algorithm that is used to solve an inverse problem is the genetic algorithm. This algorithm uses the concept of the genetic reproduction process to select the best fit model. In the algorithm, the population is representing possible model options that are to be passed or fail in the next stage.

In general, the procedure in a genetic algorithm to solve an inverse problem: the algorithm starts from an initial random population which consists of some individual. Then to get improve the estimation through a process the iteration should proceed (Vatankhah et al., 2019). At each iteration the fitness value is given for the individual then the fittest individual is selected for the next iteration to reproduce new offspring that replace the least fit individual of the current iteration. In such a way the best solution finds iteratively. Finally, the iteration procedure terminates if the misfit criteria satisfy the target misfit. In most cases especially in potential fields inversion $E[X^2]$ test has been common (Vatankhah et al., 2019).

Conjugate gradient algorithm: is used to solve a linear system of equations that have coefficient matrix with the positive definite and symmetric. This algorithm uses an iterative way

of solving the problem by inverting the coefficient matrix. In principle the solution vector obtained after applying k steps of the conjugate gradient algorithm to the normal equation $A^TAx=A^Tb$ with zero starting vector (Hansen, 2010).

The main efficiency and effectiveness of the conjugate gradient algorithm are computing the solution without the need to orthonormalize and store all the base vectors. In general, if the coefficient matrix is symmetric positive definite, the algorithm is pretty much in all forms whether about efficiency and effectiveness plus to memory (Hansen, 2010).

2.6. Tikhonov Regularization

The most successful regularization algorism of all time is Tikhonov regularization. According to numerous previous literature the method has been invented several times which means it has been updated several times for past decades this makes the method more efficient and simple to perform a complex computation in an aspect of time and memory requirement. The basic principle in Tikhonov's regularized solution is arranging the linear system of the equation to a suitable regularization system of equation (Calvettia et al., 2000).

$$(G^TG + \lambda I)\rho = G^Td \qquad (2.21)$$

Where $\lambda>0$ is the regularization parameter that determines the amount of regularization of the system, 'I' is an identity matrix that is prepared to multiply with the scalar number (λ). G is kernel matrix and d is observed data.

The regularization system of the equation described above is the equation formulated to replace a linear system of equations (Hansen, 2010). The following equation is rearranged to obtain a unique solution for the above regularization version of the equation.

$$X_\lambda = (G^TG + \lambda I)^{-1}G^Td \qquad (2.22)$$

Where X_λ is the regularized solution

The Tikhonov solution X_λ is set in the form of the Euclidian norm. This norm is used as the Tikhonov objective or cost function. The solution X_λ of equation (3.9) satisfies the minimization problem

$$X_\lambda = \min[\![\|Gp - d\|^2 + \lambda^2\|L(x - x_0)\|^2]\!] \quad (2.23)$$

Where $\|\ldots\|$ is Euclidian norm, λ is regularization parameter, x_0 is reference model and L is a matrix used to incorporate prior information.

The general form of the Tikhonov cost function has the above equation (2.23) formulation. In the case of the standard form of Tikhonov, the cost function has a formulation below (2.24), the matrix L is equal to the identity matrix (Calvettia et al., 2000).

$$X_\lambda = \min[\![\|Gp - d\|^2 + \lambda^2\|x - x_0\|^2]\!] \quad (2.24)$$

The first term of equation (2.24) is the residual norm that helps to evaluate the data misfit between observed and predicted data. If the residual norm is too large solutions obtained are not represented as a well-regularized solution of the problem. On the other hand, if the observed data contains noise and the residual norm to be too small, then the solution obtained from such a condition is to fit noise in the observed data. The second term of equation (2.24) is the solution norm that measures the regularity of the solution. In other words, it measures the degree of solution to satisfy apriori information that is incorporated in objective function through the L matrix (Hansen, 2010).

The problem associated with the strongly ill-posed condition cannot be simply solved by a least-square solution. Because the geophysical inverse problem has a nature of instability i,e the small change in data space causes a large change in model space, such nature of instability leads to upgrading simple least square to regularized solution form. When we develop the form of solution to regularized form, the most important quantities that help to regularize the solution are regularization parameters. Therefore we need to have algorithms that can compute optimal regularization parameter. This section of the paper well explored various kinds of regularization selection algorithms that have been commonly used in a related subject.

L- Curve criterion: The regularization parameter highlighted above in the Tikhonov algorithm is a too indispensable quantity to carry out regularization for the ill-conditioned inverse problem. For the sake of understanding how the L curve works and to clarify the mathematics behind the L-curve criteria which show the behavior of solution with the corresponding choice of regularization parameter λ is well described in this section of the paper. One of the important

and well-known regularization parameter selecting methods is known as the L-curve criterion (Calvettia et al., 2000). The L-curve criterion has been broadly used in several previous related kinds of research that are worked on solving the ill-conditioned inverse problems. Because of its simplicity to numerical analysis and has good efficiency for a different scope of the study area. The L-curve criterion is used to compute the optimum regularization parameters to stabilize the objective function that solves for minimization of solution and residual norm simultaneously. The main role of the L-curve is to keep the balance between data misfit and solution to recover a reasonable model subject to the expected value of residual (Calvettia et al., 2000). In general, this L-shaped curve is a plot between solution norm and residual norm in the log-log scale. L-curve consists of two features: one is a vertical section that is completely dominated by regularization error due to too much assignment of regularization parameters. The second is a horizontal section that is fitted with the noise of observed data. In general L curve plays a significant role in the process of inversion to obtain the best regularization parameter that can bring a plausible model by controlling the contribution of residual norm and solution norm. On other hand the corner of the L –curve is a feature associated with target information that is recovered from the curve where the optimum regularization parameter locates. In principle, the selection process lies on the following two expressions which are called solution and residual norm. The residual norm monotonically increases in λ whereas the solution norm monotonically decreases in λ (Calvettia et al., 2000).

- Residual norm

$$P(\lambda) = \|Gp - d\|^2 \tag{2.25}$$

- Solution norm

$$\xi(\lambda) = \|L(x - x_0)\|^2 \tag{2.26}$$

The corner point of L shaped curve is represented by the following expression.

$$C(\lambda) = \left(\frac{1}{2}\log_{10}P(\lambda), \frac{1}{2}\log_{10}\xi(\lambda)\right) \tag{2.27}$$

Generally, the process of parameter selection for regularization in practice is automatically done by a computer system.

Discrepancy principle: The discrepancy principle is one of the well-known regularization parameter selection algorithms. This approach was first invented by Morozov sometimes it is known as Morozov's discrepancy principle (Richter, 2016). The basic assumption behind this approach is; only an approximation b^{δ} to the data b is at hand, and that its error can be bounded in the form $||b - b^{\delta}||_2 \leq \delta$ with $\delta > 0$ known Morozov's discrepancy principle for choosing the regularization parameter λ with being replaced by b^{δ}. The following condition is helped to choose regularization parameter λ:

- ✓ Choose $\lambda = \infty$ if
$$||b^{\delta} - AX\infty||_2 \leq \delta$$
- ✓ Choose $\lambda = 0$, if
$$||b^{\delta} - AX_0||_2 > \delta$$
- ✓ Otherwise choose the unique value λ, for which
$$||b^{\delta} - AX\lambda||_2 = \delta$$

Generally in this approach regularization parameter is chosen depending on the error level δ in the observed data (Richter, 2016). The above-listed condition is directly taken from Richter (2016)

Generalized cross validation: This approach is another form of regularization parameter selection algorithm based on the statistical nature of the prediction error. The method works in the way of searching regularization parameters that can minimize the prediction error. In generalized cross validation, there is the curve plotted between vertical section and horizontal section that consists of a series of numbers for select regularization parameter to be obtained from when the prediction error is being minimized (Hansen, 2010). The optimal regularization parameter is obtained from the plotted graph when the parameter lies nearby the transition zone between the flat section in a horizontal direction and steep in the direction of a vertical axis.

2.7 Review of Previous Work Related to Gravity Inversion

The whole area of interest for the study is sufficiently covered or mapped by gravity data in the required space for geoscientific investigations that help to study subsurface geology. This adequate amount of data leads a geoscientist to further investigate the complicated system of subsurface geological structure. A lot of gravity-related works have been conducted to enhance

the insight toward the concealed subsurface geology of the region. Mainly these studies focused on determining moho depth, modeling crustal structures, and other closely related issues. Most of these studies are made their focus on the Ethiopian rift system because the area of interest has been exposed to different geodynamic events such as active volcanoes, plate tectonic motion, and other related apparent phenomena. This and other related issues have been enforced from local up to the global researcher to make their focus on investigating about crustal structure condition of the region.

Mahatsente et al. (1999) had studied 3D modeling the crustal structure of the main Ethiopian rift from gravity data. The author was used to show the geometry and density distribution of the garben. In a general sense, the study portrayed the density distribution of the garben using a computer programming package. On the other hand author, Tiber et al. (2005) had performed gravity inversion to determine various crustal structures which underly beneath the east African rift system including the Afar depression. In the study, the author has performed gravity inversion on spectral-domain and used an iterative inversion approach to determine moho depth, crustal thickness, and lithospheric thinning. These and other numerous geo-scientific researchers have conducted gravity and other geophysical inversion techniques to determine or model crustal structures of the great east African rift system. On a similar subject matter, a significant study has been done by geo-scientific researchers Cornwell et al. (2005) and other several researchers.

However as observed from an extensive review of previous articles, all of the studies have been performed on a determination of crustal structures, moho depth, lithospheric condition of the region in different dimensions and viewpoints. In addition, the general approximated density of the structures was also estimated at different layers of the crust.

In general sense gravity inversion for mineral exploration did not conduct in the range of scope of the study area. So to dedicate this approach to the application of mineral exploration on the target region, various articles have reviewed that are helped to perceive the feasibility of the context of information to be recovered, how much effectively represent the underlying geology of the target region. In addition to this, the computational efficiency of the method have examined. Numerous articles have been published on the method of the application of mineral exploration. And critically reviewed such kind of work to examine and adopt in my context. The

3D gravity inversion using graph theory and equidistance function was carried out to detect mobrun ore body (Vatankhah et al., 2019). As the study demonstrated, the maximum extension and geometry of the ore body had recovered successfully. In addition, the study can be justified as good agreement as it requires being in between the recovered output and drilling borehole information.

The research worked at Geju tin-copper polymetallic ore field in Yunnan province and Tongshi goldfield in western Shandong have used Bouguer gravity anomaly to recover a mineral deposit concealed under the region of study (Chen, et al., 2018). Mainly the study used the bidimensional empirical mode decomposition technique to investigate subsurface anomalous mineral of the region. Finally, the study result showed the spatial distribution relationship between different intrusive bodies and mineral deposits. Another study that had used the gravity inversion technique is carried out in Egypt, which is a comparative study used to evaluate a different method of gravity inversion for mineral site exploration. Thus are gradient method, particle swarm optimization techniques, and Werner deconvolution (Essa and Elhussein, 2018). The real data obtained from Egypt was used to test the feasibility of the methods. The article had demonstrated the efficiency of the methods to recover reasonable output if we used sufficient constraint and prior information about subsurface geology.

On other hand, Yaoguo and Oldenburg (1998) had conducted 3D gravity inversion at health steel stratmat copper-lead-zinc deposit in northern New Brunswick. The focus of the study is to test the applicability of gravity inversion using two different methods: directly inverting gravity data and by transforming gravity data to pseudo magnetic data via Poisson relation. Generally, the strength of this study is clearly illustrated how we can use the system of the equation to obtain meaningful or reasonable information from inversion. Mainly two basic cases here is to improve the effectiveness of inversion result, the first one is incorporating geological constraint in the inversion process, the second one is an adequately defined objective function that can allow various constraint to incorporate.

Chapter Three

3. Methodology

3.1 Description of Study Area

The geographical location of the study area is between in the range of 4.6^0 N – 6.2^0 N in latitude and 38^0 E – 40^0 E in longitude (nearby southern greenstone belts of the Ethiopian rift system). The topography of the study area lies south of a central high plateau that is bisected by the east African great rift in northern and southern highland. The higher plateau of the southeast of the rift system is a high elevated area of the region, the northern and southwest corner of the study area has topography of high to moderately elevated. The low land region found in the study area covered from center to southwestern margin. The average elevation of the study area is around 1476m above MSL. Minimum and maximum elevation lies approximately in the range of 680m to 2887m above mean sea level. The topography of the study area shows a highly diversified terrain configuration.

Volcanic rocks in the region of study are more associated with the great African rift system that extends to Mozambique for 4000km. Such kinds of rock are mainly lying in the series of Ethiopian rifts from the eastern margin of the system (Afar) via crossing the central plateau to ward Sothern edge of Ethiopian territory. the mineral resource associated with volcanic rock across the rift of Ethiopia is included soda ash epithermal gold, diatomite, bentonite, salt, sulfur, and pumice (Tadesse et al., 2003).

Specifically, local geology covered in the region of study (geographically located in the vicinity of central to the southern margin of Ethiopian rift system is in the range of 4.6^0-6.2^0N and 38^0-40^0 E) is described as follows. The quaternary tertiary rift sediment and volcanic rock are covered around the northern border of the study area. The tertiary highland volcanic is covered around northwestern and it extends the center toward the southern margin of the study area. On the other hand, quaternary cover (undifferentiated) is extended from the west to southwestern margin and southeastern border of the study area.

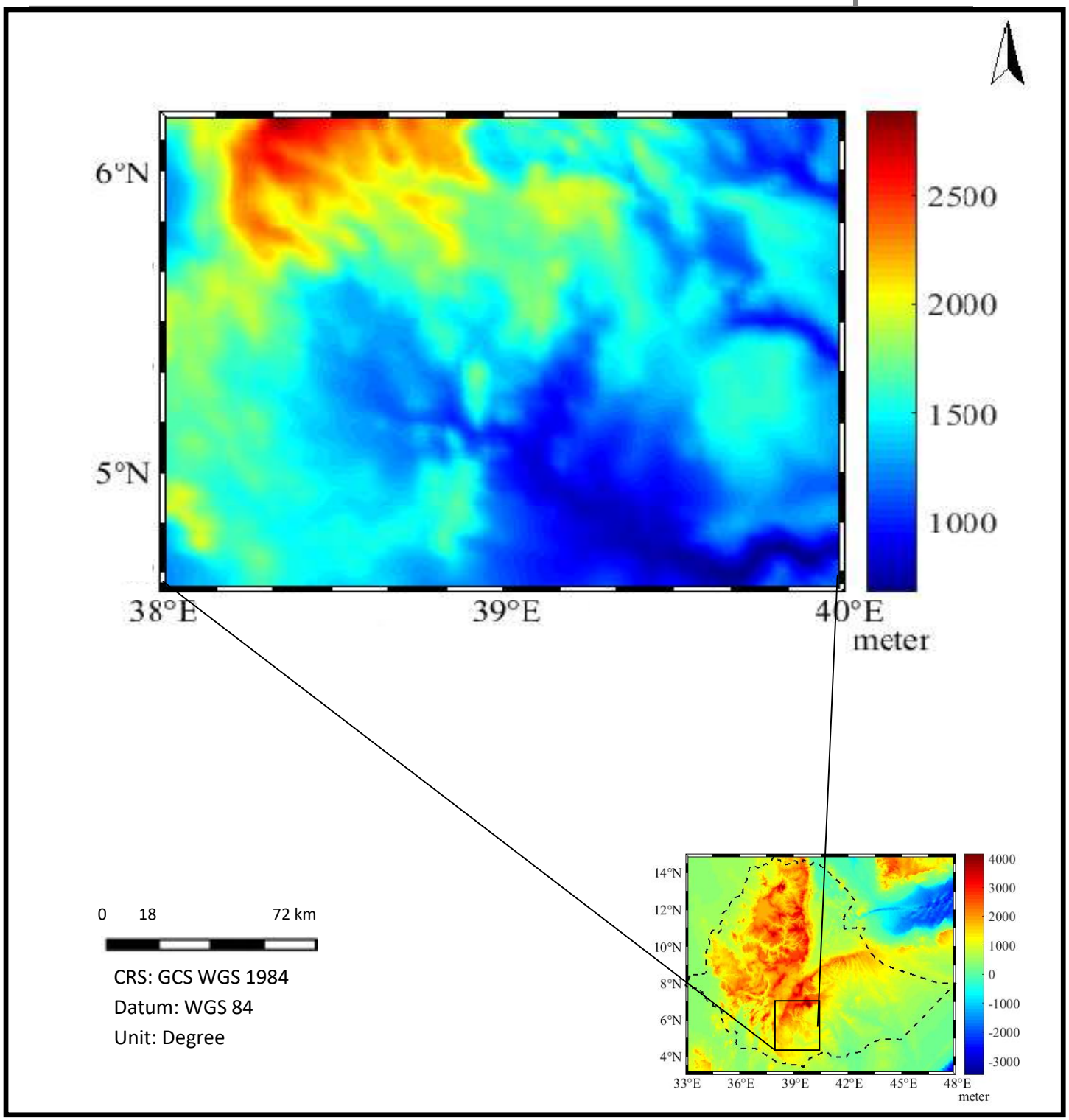

Figure 3.1 *Geographic location of study area*

Other more dominantly covered at the central region of study is Archean type. In addition, it covered eastern margin elongated to a south ward. Mesozoic sediment is covered at the northern corner of the region and extends toward the center of the region with a narrow dimension, which is adjacent to quaternary-tertiary rift sediment in the northeastern direction and Proterozoic metamorphic in the south eastern direction (Tefera et al., 1996).

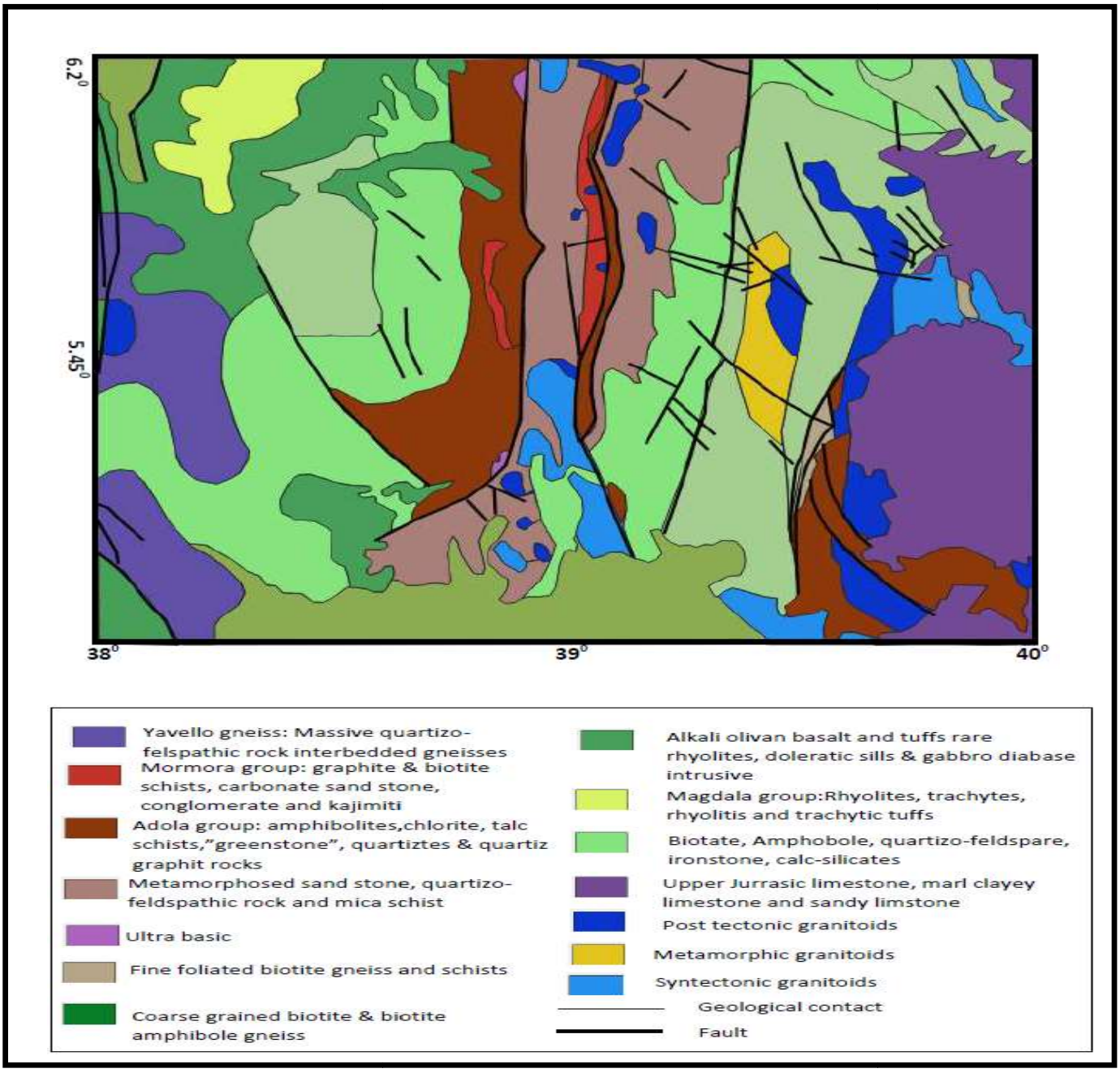

Figure 3.2 *Geological map of study area*

Various mineral types has been discovered in the region of interest thus are abundantly gold occurrences are well known at Lege Denbi, Mormora, Shakaro and Adola area. Other kinds of mineral that associated with geological event are existed for instance, Iron ore, Cobalt, Nickel, Chrome, and Tantalum. The following figure shows the description of metallic mineral withrespective location in the region.

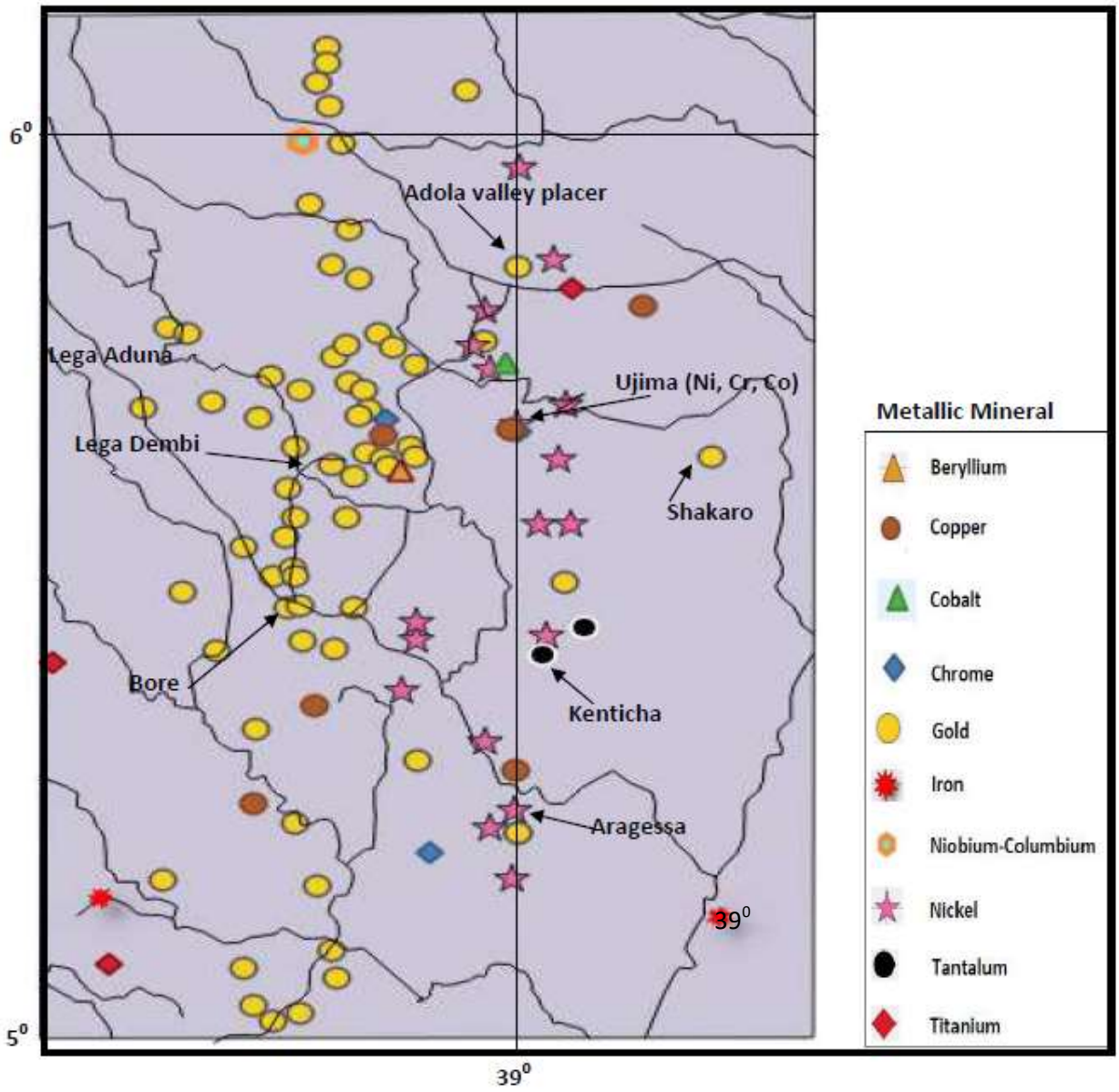

Figure 3.3 *Mineral potential map of study area (Tadesse et al., 2003)*

3.2 Data Used

The basic material and data that used in this study are described in this section of the paper. The central data is gravitation acceleration of the region that is used as input data to achieve the specified objective of this study. According to the national airborne gravity acquisition programs' report that prepared by Danish National Space Center DNSC (Olesen and Forsberg, 2007), an airborne gravity survey was carried out in the entire territory of Ethiopia. The survey was covered 90 000km flight distance that is consists of 92433 data. After the acquisition process was conducted, all necessary correction was performed and prepared to use various geo-scientific purposes. For this study, the gravity data is extracted from the above described airborne data for the extent of 2 x 1.7 degrees at the southern rift system in the range of 38-40 degree in east direction and 4.6-6.2 degrees in the north direction.

Another piece of data that is used for this study is a geological map of the region. The detailed geological map prepared by Ethiopia geological survey is obtained from Ethiopia geological survey main office Addis Ababa. The role of the data for this study is to understand the underlying rock type, geological evolution, and other related features that are used for incorporate apriori knowledge about the study region of interest.

The density of the rock in the area of interest is another important data for constraining the inversion process. The approximated density of host rock is taken as the initial density to preserve the inversion result from the unrealistic output. CRUST 01 model is the density model downloaded from the website is used for constraining inversion.

The platform to process data, execute inversion and another graphical visualization is mainly done by Matlab software package. Various functions, code, and tools are used to calculate kernel matrix, execute inversion, to create and display images. The Matlab programming software code package prepared by Hansen (2010) is used with a little bit of modification for executing inversion. To calculate the big size kernel matrix, Matlab code are written in an appropriate form to the case of this study. Other software that used to various map visualization and data preparation is SAGA GIS which is the extension of QGIS. The following table summarizes the data types and their source that has been used in the current study.

Table 3.1 Summary of material used

No.	Data type	Purpose	Source of data
1	Airborne gravity data	Input data for inversion	Ethiopian gravity survey (2006 to 2008)
2	Earth crustal model(CRUST 01)	A priori knowledge	(Bevis, 2017)
3	Geological map of Ethiopia	To interpret and weigh the model	Institute of the geological survey of Ethiopia(IGSE)
4	Borehole information	To interpret & validate	Previous documents
5	Digital elevation model	To extract elevation of terrain	USGS
	Software used in the study		
1	Matlab software	For numerical computation	Mathworks
2	QGIS	For filtering and displaying map	
3	MS excel work shit	For data analysis	MS Company
4	MS word	To prepare document	MS Company

3.3 Data Correction

The gravitational acceleration measured at the observation point by gravimeter is the acceleration due to the underlying mass distributions of the earth and other different factors nearby the observation station. The measured raw data consists of gravitational acceleration because of several factors mention below. In a general sense, we can segment the contributing factors of the observed gravity value to facilitate the data to be suitable for investigating the situation of subsurface geological nature of the earth. The measured gravity on or above the earth surface is the responses of the following contributing factors: I) the mass of ellipsoidal approximated earth, II) the topographic mass effect, III) the distance of measurement point from the causative body, and IV) the error involved due to imperfection of instrument and other error due to natural environment. The basic task that is required to involve under investigation is removing other unnecessary signals from the raw data to obtain only target signals that are necessary to further analysis in the study. The first step of data processing is to carry out a correction for errors that are involved in measurement quantities due to instrument drift and correction tide effect. After removing the erroneous section of data the next task is applying corrections for the effect of unwanted signals that are described above. Free air correction which applies for the effect of height of measurements that deviate from the reference surface and in the assumption topographic mass in between is neglected. Another correction that applies for the mass effect of topography that was neglected in the case of free correction is called simple Bouguer correction. In such a case topography is assumed to be horizontal infinite rock slabs that have a constant

thickness and density. On other hand due to the constant approximation of the Bouguer plate being used in simple Bouguer correction, it intended to consider truncated residual terrain because of the reliefs up and down in the vicinity. This correction applies for relief deviation up and down from Bouguer plate is commonly known as terrain correction. After all those corrections have been made, the final output is combined Bouguer gravity anomaly which is used as an input variable to the inversion process. The detailed procedure of all corrections described above is explained in the next section of the paper.

Free air correction: applies for the gravity change due to observation height difference from reference datum ellipsoid. The basic assumption in free-air correction is considering the space between observation points and reference datum as mass free space, this means neglect the mass (only air present)in between hence its' name is called a free-air correction. In such an assumption the rate of change of gravity in mgal per mater has been calculated and used in the current study (0.3086mgal) as described under the theory section.

The procedure that is used to get free air anomaly is: first normal gravity at ellipsoid calculation has done using the international formula of GRS80 ellipsoidal model. Then the next task was calculating upward continuation factor or free air correction with respective elevation at the observation station. Under this process, the elevation of flight height is obtained with gravity data from the source. After preparing individual variables (observed gravity, normal gravity, and free air correction) the next task was simply reducing the ellipsoidal gravity effect from observed gravitational acceleration and then adding the result with the effect of altitude at the individual observation station. The final result obtained from the process is called the free-air gravity anomaly of the region. In general, the algorithm to calculate free air anomaly is described in detail under the theory section.

Bouguer correction:. Since the mass of topography has a significant effect on gravity, the Bouguer correction is required to apply after free air correction has been made. The assumption involved in Bouguer correction is computing the contribution of rock mass of topography by approximate as infinite horizontal rock slab as described and illustrated under theory section. The consideration during computation of this correction is the constant thickness of slab for a point and density of rock slab which is 2.67g/cm^3. Then Bouguer correction was carried out according

to the general formula (BC=0.0419ρH). Finally, we obtain the correction which is caused by topography that approximated as Bouguer plated. The result obtained from such a process was applied on free air corrected gravity anomaly to get a simple Bouguer anomaly. The final result of complete Bouguer anomaly (CBA) was obtained after adding terrain effect on simple Bouguer.

Regional residual separation: In the procedure of data preparation stage the previous topic explained about the calculation of gravity anomaly that is used for retaining target signal this means removing the signal which is not necessary for investigation objective of the study. Then the next step is to narrow down the extent of a signal based on its wavelength. Separation of regional effect from total gravity anomaly is the basic and important task to obtain the signal due to relatively shallow anomalous body. The interest of this study is to explore mineral resource that occurs at shallow depth. Therefore the signal of far effect or high wavelength signal becomes an error to this study so removing such a signal is reasonable. The separation scheme is high pass filtering of gravity anomaly signals. That means removing the high wavelength component of the signal. To terminate the separation or filtering process the knowledge about underlying local geology and regional geology have a significant role. With the help of previous geological and geophysical information, the target relevant signal of the study is identified so that based on such process the residual target anomaly is obtained. The basic tool that is used for the separation or filtering process is SAGA GIS geo-scientific software.

3.4 Inversion Methodology

In this section, a brief description of all progress involved under 3D gravity inversion based on Tikhonov regularization theory is discussed coherently. After data processing was accomplished the next task was discretizing the target model space or subsurface earth that is appropriate to carry out the inversion process. Subsurface earth is approximated as a finite number of rectangular blocks. Mainly such approximation is selected as suitable because every rectangular block used as a model cell has an edge-to-edge connection without any gap between individual cells. In addition, such a discretization approach has been described as an efficient approach than others we have explored in the previous article under the review literature section of the paper. Mainly the assumption of the method lies on calculating the response of individual rectangular prism to the gravitational attraction that is measured out of the model domain. The integral of the

contributions of each prism(model element) produces the observed gravity field this means the sum of the gravity effect of individual prism gives the gravity effect of the whole model element(model block). The gravity attraction of measured at station 'i' is the result of the contributions of the whole masses of underlying prisms. The model elements or each prism are considered to be constant volume, density, and dimension in all x, y, and z-directions. In general, the governing mathematical equation that helps to formulate the relationship between gravity anomalies with anomalous density distribution in a discrete fashion is in detail described under the theory section in chapter two.

The first step before went to inversion was the preparation of the geometrical center of individual cells' node location. The geometrical center of the individual cell was determined by adding the half cell size on the starting location of a model then the next node of all cells was obtained by adding the cell size up to the boundary of the model. In such a way the location of the model cells was determined. After determining the model location and observed data location the next task that was accomplished is the formulation of a kernel matrix that mathematically relates data and model as a forward operator.

The kernel is a matrix that is obtained from the fundamental relationship of model space to data space that can allow for extracting the sensitivity of the model element to the data. The detailed issue of kernel matrix formulation is arranged and put in an appropriate context for the study of interest as follows.

The kernel matrix is a matrix that is used to relate gravity observation at a particular station with the model element which exists in the entire territory of the model space. Mainly the formulation of kernel matrix is based on the parameters that directly relate gravity anomaly with causative anomalous density in the vicinity. The basic factors or variables involved during the formulation of kernel matrix are: i) well define the simple geometrical shape for a differential element of the model (rectangular prism) and determine the dimension of each model cell in an appropriate way that is suitable to extract target information of the study. ii) The distance between the geometric center of the cell and the observation point. iii) Spherical angle between the observation points and the geometric center of each cell.

Based on the above-defined parameters or variables the sensitivity of the jth cell to ith observation is established to calculate a big size matrix that holds the relationship of observed data with target model space. In principle, the necessity of kernel matrix formulation is obvious as explained in the previous section of the paper it holds the general mathematical concept of density-gravity relationship that helps as a basic tool for mapping these two quantities from one to another. The matrix dimension is N (number of data points) by M (number of model parameters) which helps to calculate the influence of each model cell on observation.

To easily apply to numerical computation the Green's point mass gravity kernel described under the theory section are adopted (Liang et al., 2014) in the spherical coordinate system as a form of equation below:

$$G(N,M) = \frac{\mathbb{K}r^2\cos\varphi\Delta r\Delta\varphi\Delta\lambda(r'-r\cos\Psi)}{l^3} \qquad (3.1)$$

Where G (N, M) is a kernel matrix that has a dimension of N (number of observed data) times M (number of model cells). The dimension of the model cell in radial, latitudinal and longitudinal directions is $\triangle r$, $\triangle\varphi$, $\triangle\lambda$ respectively. The universal gravitational constant is $\mathbb{K}$, the spherical angle is (Ψ).

Based on the given equation (3.1) the sensitivity of each cell to i^{th} observation is depends simply on the size of cells and the distance between the geometric center of the cell and the observation point. Specifically, kernel matrix was applied for two basic purposes in the method of gravity inversion the first one is for the basic purpose that have described above i,e directly relating individual model with every data point. The second function was to carry out the L-curve that is used to select optimal regularization parameter. This has been done after decomposing kernel matrix G in to right orthogonal matrix, left orthogonal matrix, and singular vector.

After kernel matrix formulation is accomplished the next task was preparing appropriate functions that are involved under Tikhonov regularization theory. Various kinds of methods that help to solve an inverse problem were reviewed from different literature that is well described under the theory section of the paper. After examining the advantages and disadvantages of the algorithm those are mentioned under the theory section Tikhonov regularization algorithm was selected for several reasons.

3.4.1 Tikhonov Regularized Solution

As described in the theory section several approaches are used to solve the inverse problems. All have their advantage and disadvantage based on the quality of the solution, efficiency, and memory requirement. Based on such criteria Tikhonov regularization approach has been chosen by some geophysical studies. And the performance of the method has been evaluated in the various casa study as we have seen from various geophysical studies.

The inversion process in this study is mainly based on the Tikhonov regularization algorithm for minimizing the specified objective function. The Tikhonov cost function is the main tool in the regularization process in the form of an objective function to be minimized. Mainly this objective function is optimized automatically with the help of Matlab code that is written for the purpose of computing the function numerically. The basics of inversion of gravity anomaly in this study lies in solving the problem of nonuniqueness in a form of setting appropriate objective function that is required to be regularized.

While regularizing the Tikhonov cost function, three main components should be involved and considered in the analysis.

- Data misfit norm
- Model norm(model objective function)
- Choice optimal Regularization parameter

I. Data misfit norm

Data misfit norm is one basic component or part of the procedure of the method. The basic role of the data misfit norm is to deal with the statics of mismatch between observed and predicted data. The misfit norm here used in the method is the L2 norm which is Euclidian length. The L2 norm or Euclidian length helps to determine the sum of the square of residuals between observed and predicted data. In the process of minimizing the objective function, the role of a residual norm is to minimize the norm subject to target misfit value. The target misfit value is obtained from the general error statistics of the data (standard deviation of the data) with the corresponding relationship to its norm. In general term, this section describes the mismatch between observed and predicted data while minimizing both norms simultaneously in the regularization process.

The main significance of the data misfit norm is to incorporate the noise level in the minimization process. On other hand, it helps to estimate the noise level in the data with trial and error repeating the procedure if we have no noise information.

II. Model norm

The model norm is a way of incorporating prior information and appropriate weighting factor that helps to recover compacted and smooth outcomes or models. The model norm is designed to allow prior information to be incorporated in the minimization process. In this study, the model norm comprises two basic variables those are model parameters that are to be recovered as a solution and the model weight that are described in later section. Finally, the norm is involved in the regularization process to measure model perturbation. The type of norms used in this study is the L2 norm that measures the model perturbation. Mainly the quality and resolving capacity of the final model (density contrast) depends on the amount of constraint to be involved in the model norm.

III. Choose optimal regularization parameter

This section is the third important component involved under Tikhonov cost function that helps to regularize model perturbation. The regularization parameter that to be selected are involved in objective function; it is a small positive constant. As described under the theory section, the detail about methods of selecting optimal regularization parameters are mentioned; L-curve criterion, discrepancy principle, and GCV. From those algorithms, L-curve principle is selected for this study because of simple to implement and it has been popular in similar previous studies.

3.4.2 Formulation of Prior Information

Involving additional information observed from geophysical, geological, and other physical observation in the minimization process can recover better and reasonable solutions. Because when we give more apriori information about an underlying situation to the model norm as a weighting factor, the possibility of getting a reasonable solution is high, on other hand getting an unreasonable solution is diminished. Therefore the apriori information about the region of interest should be involved even if the amount is small; it can bring somehow significant improvement in the model parameters' characteristics or nature. In this study, two types of additional information are included in the model as a form of model weight.

The first one is the depth weighting function that helps to reduce the decay of gravity field kernel with the depth just like happen in other potential inversions. During gravity inversion without depth weighting, the resulting density is concentrated at shallow depth irrespective of real depth. This problem is recently solved by applying depth weighting as verified in some previous studies. That has a significant role to recover information at an appropriate depth. Therefore this is reasonable to use depth weighting in the current study.

The way of applying depth weight in our context is first to compute the vertical distance between data observation height and model cell then normalize it to make a maximum value 1 and then convert the Mx1vector to M x M matrix. Finally, this matrix is involved in the model norm.

The second model constraint is model weight extracted from the underlying geology of the region. Firstly the general geology of the region is digitized in QGIS then given Id to the rock with similar physical properties this means the rock that has close range density value and age. Then finally the reclassified weighting factors are involved in the inversion.

Another constraint is the data weighting matrix that is the way of incorporating error standard deviation in data misfit. It incorporated in the form diagonal matrix the element of the matrix is the reciprocal of the standard deviation of data noise.

3.4.3 Numerical Solution

For numerical computation, the required input variables are assembled in a form appropriate to execute. Input data that to be inverted is prepared as a vector of gravity anomaly with corresponding geographical location. The location data is used for calculating the kernel that determines the relationship of gravity anomaly with underlying model space. The second input parameter is a kernel (G) matrix which determines the sensitivity of each observation to each model element. The third input variables are the weighting matrix: wd and wm are data weight, model weight. Regularization parameter selected using L-curve criteria. The final matrix formulation after minimized Tikhonov cost function is given in equation 3.2. Finally, the numerical calculation of the matrix is accomplished using a conjugate gradient.

The first task in the numerical calculation is a computation of matrix B as a sensitive matrix its dimension was M x M (M is the number of the model cell). The next action is computing the l matrix according to the formula described in the appendix.

$$B \triangle\rho = l \qquad (3.2)$$

Where: $\triangle\rho$ refers to density contrast (model perturbation) and

After matrix B and l are obtained the next task that has been processed is to carry out inversion with the help of the fast and simplest method called conjugate gradient. In the end, the model parameters obtained from inversion is the density contrast of the individual model. After obtaining the density contrast model from inversion

Ultimately what we can perceive from the model is; 1) density contrast of underlying geology that reveals the extent of perturbation relative to the reference model.

3.4.4 Validation of Result

At the end of the inversion process, the next thing is the validation of whether the recovered density distributions are acceptable or not. The process is done based on assessing the results how much agree with the known information. The comparison process is done with the borehole information, geological and mineralogical situation of the region. After the accuracy of the result is assessed with those facts about subsurface geology, the result that has good consistency would be used as the last model for gravity inversion.

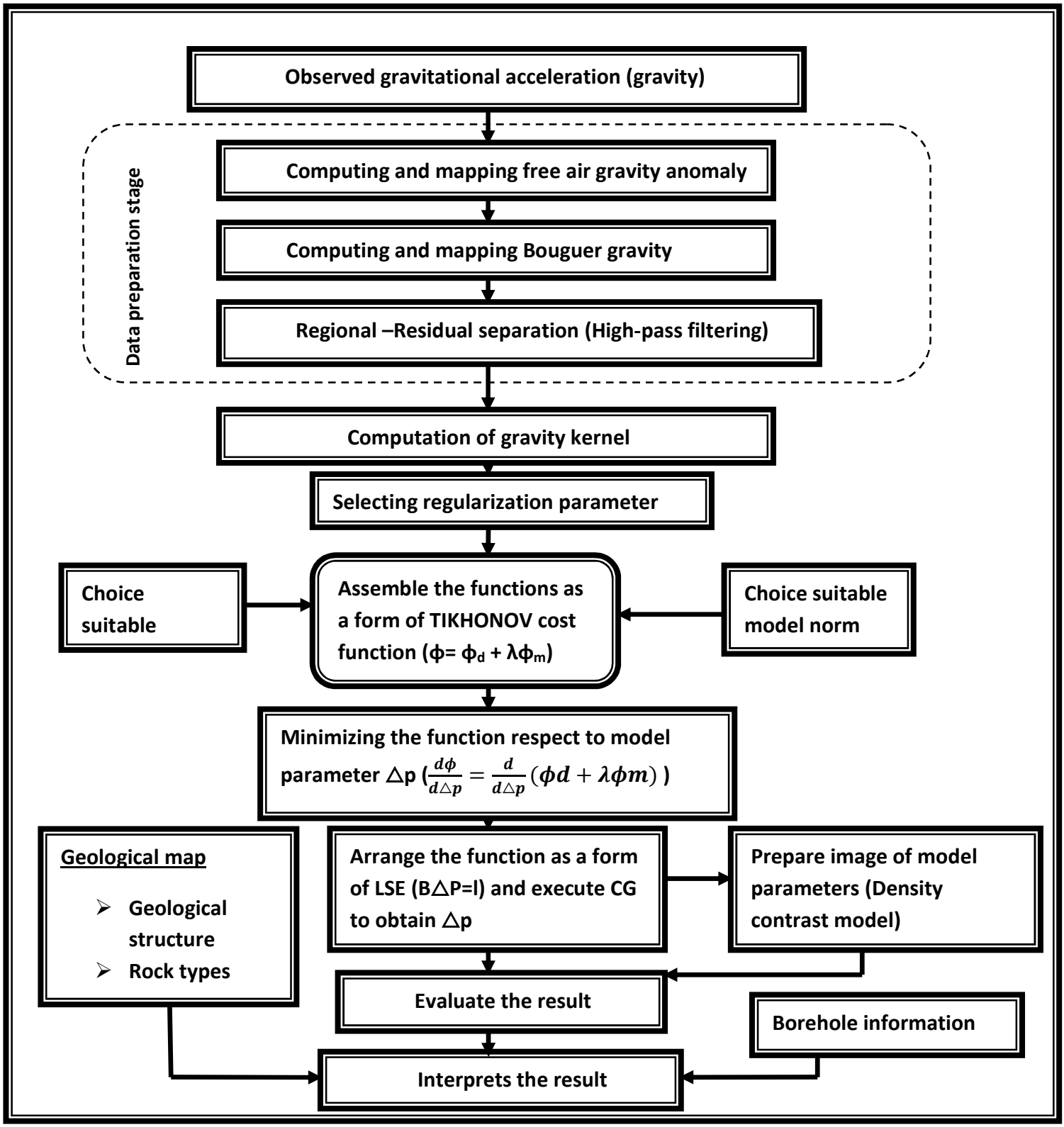

Figure 3.4 *General workflows*

Chapter Four

4. Result and Discussion

4.1 Complete Bouguer Anomaly

Bouguer anomaly map is obtained after making necessary corrections that are described under the method section. In general term, Bouguer anomaly map shows the lateral density distribution of the underlying geology of the observation area. Therefore this anomaly is fundamental input parameter to deal with the density of subsurface geology.

The Bouguer anomaly map in Fig. 4.1 is the result after removed unnecessary signals from observed gravitational acceleration. In this study total of 5250 data point is used to compile this map. The procedure to reduce gravity and to prepare the grid was carried out in Matlab software.

Bouguer anomaly map of the study area showed the trend of high-medium-low gravity anomaly region. High gravity anomaly region is revealed around the southern and southeastern margin of the study area. And the magnitude of the high gravity anomaly in this region is -91mgal. The medium Bouguer gravity anomaly scored in between as we can see the medium gravity anomaly occurred between in the range of high and low gravity anomaly. The least Bouguer anomaly was revealed around the northern and north-western margins of the study area. The magnitude of the lowest Bouguer anomaly in this region is -190mgal. In general, this map shows the total Bouguer anomaly that involves the regional and the local effect. Therefore for extracting the target anomaly we have to separate it into the regional and residual forms. As far as the main target of the study is recovering density contrast of near features, it is necessary to extract the residual anomaly. The high negative Bouguer gravity anomaly obtained around northern and northwest are associated with mountainous region of study area. In contrast less negative region is obtained around low lying region of study area.

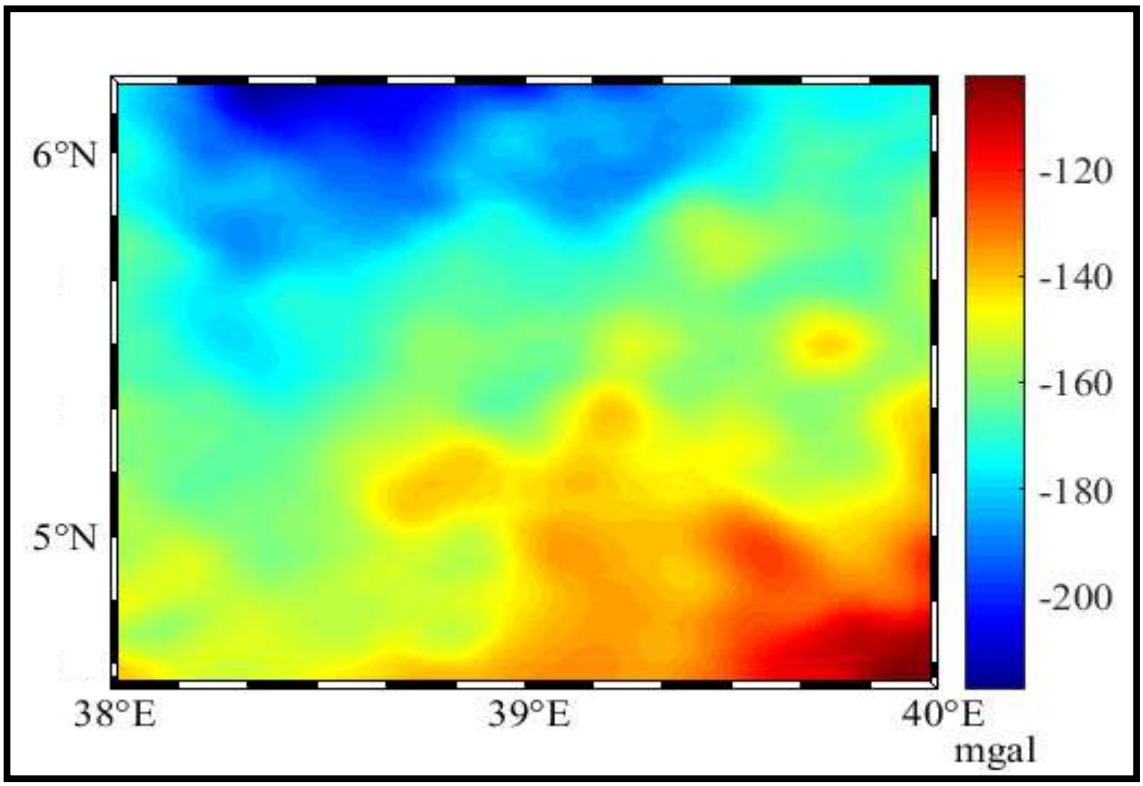

Figure 4.1 *Complete Bouguer anomaly map*

4.2 Regional Bouguer Anomaly

Regional Bouguer gravity anomaly shows high wavelength component of Bouguer anomaly that depicted at Fig. 4.1. The long wavelength component means gravity anomaly because of deep source mass. Therefore regional Bouguer gravity anomaly reflects the regional disturbance due to deep-sited geological anomaly in the region.

The regional Bouguer anomaly maps are obtained after carrying out the filtering process in SAGA geo-scientific software. The separation or filtering procedure is repeated until the regional effect is completely separated from the Bouguer anomaly map to get target local anomalous gravity.

As we have observed the trend of gravity anomaly at the regional Bouguer gravity map (Fig. 4. 2), the regional high anomalies around SE smoothly decrease toward the NW direction. This smooth variation indicates a low frequency or high wave feature of the signal.

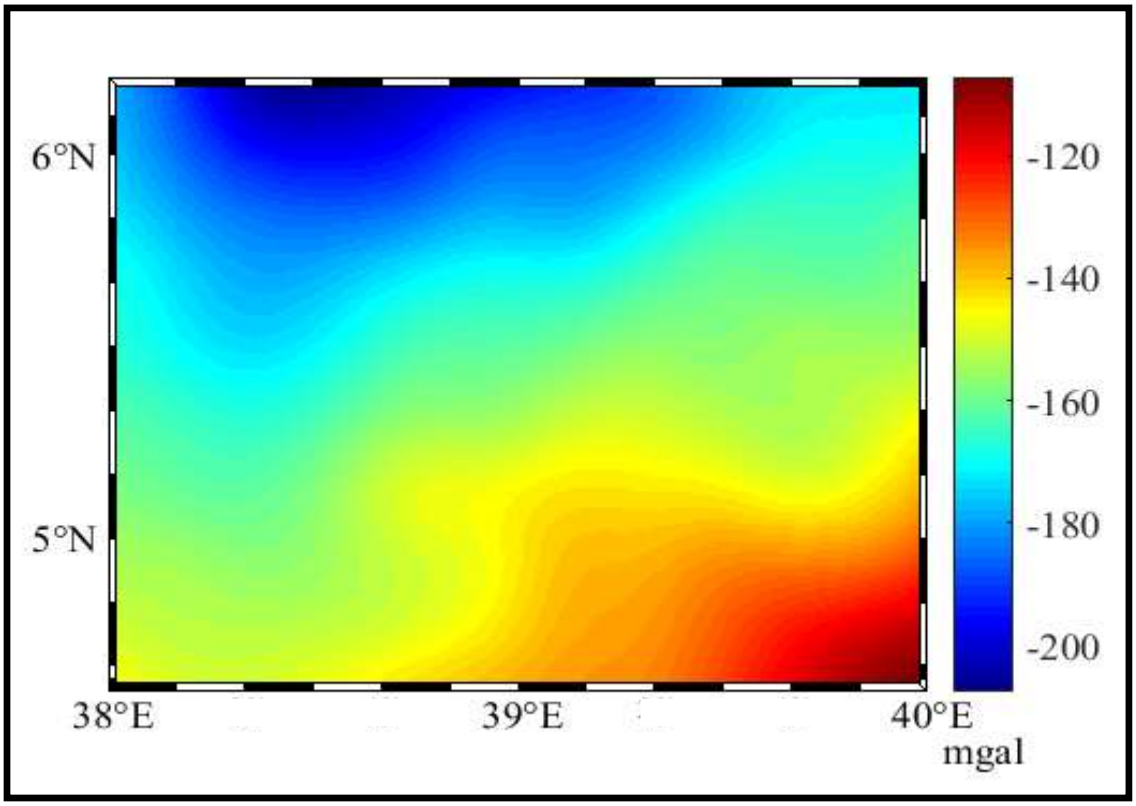

Figure 4.2 *Regional Bouguer anomaly map*

4.3 Residual Bouguer Anomaly

Residual gravity anomaly is a Bouguer anomaly after separating the regional effect or high wavelength component. This map shows the high-frequency components of the Bouguer gravity anomaly. Therefore this local variation of gravity anomaly directly indicates shallow sited geological anomaly or shallow depth source mass.

The residual anomaly map revealed in Fig 4.3 reflects a local variation of gravity due to the underlying geological anomaly of the region. The range of residual gravity anomaly observed after separation is between -10 to 10 mgal.

In general residual anomaly map revealed in Fig. 4.3 is used as the final input variable or parameter to carry out inversion.

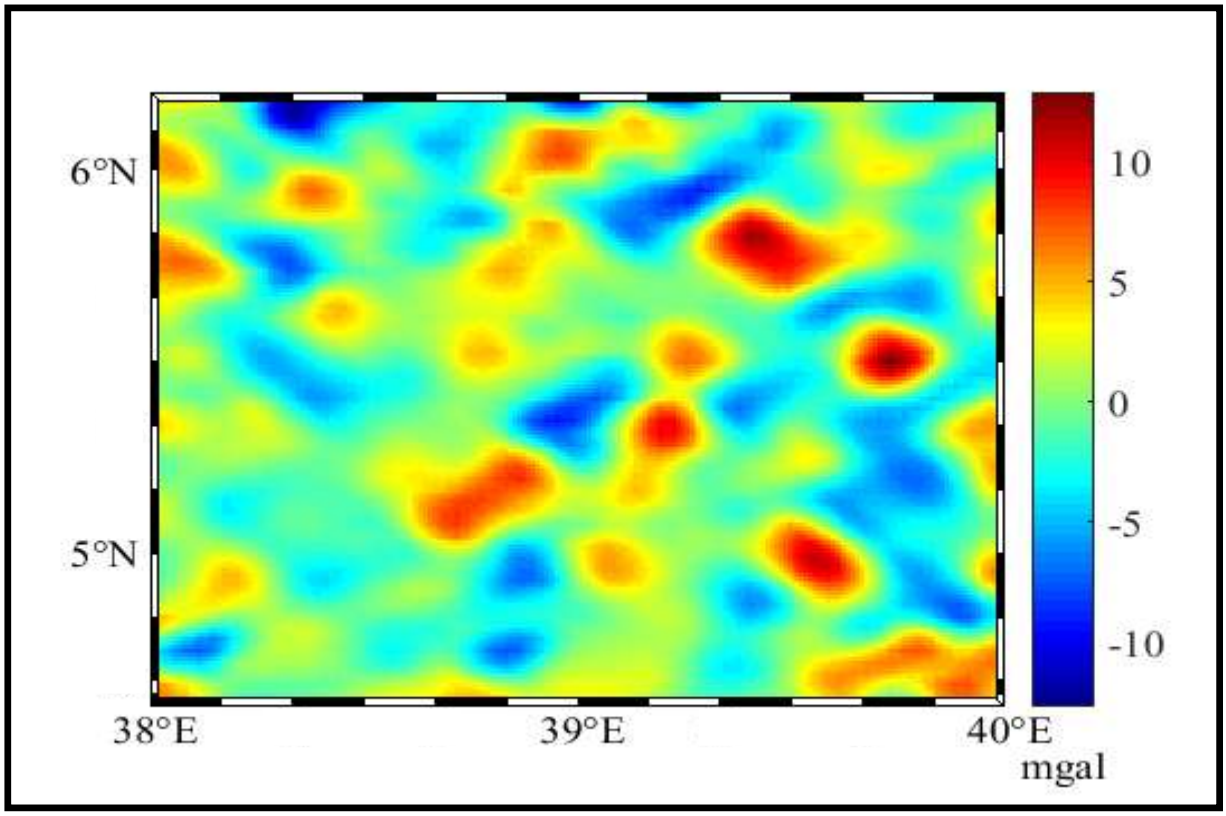

Figure 4.3 *Residual Bouguer anomaly map*

4.4 Gravity Anomaly Inversion

This study examines whether gravity data can be used to recover the ore bodies and subsurface geological structure of the southern greenstones gold deposit formation. The gravity data that were used for this investigation is airborne gravitational acceleration data which covers the spatial extent of 2^0 in the east-west direction (from 38^0 to 40^0 E) and 1.7^0 in the north-south direction (from 4.6^0 to 6.2^0 N) nearby southern greenstone gold deposit region. The observed gravity data corrected for all necessary correction that helps to remove unnecessary signal for target investigation. The final residual anomalies were gridded at regular spacing 2.5 km x 2.5 km in the X-Y direction. A total of 5250 data locations were used to invert a model. The model space is constructed from small size rectangular prism or cells with constant density contrast. The dimensions of the model elements or individual cells are discretized as 2.5 km in the east direction and 2.5 km in the north direction and non-uniform discretization in a depth direction.

Various inversion parameters were used to carry out inversion of residual anomaly thus are model weighting parameters, data weighting factors, depth weighting function, and regularization parameter.

On the other hand depth weighting functions were used to constrain the inversion algorithm that helps to prevent unrealistic concentration of anomalous body to a shallow depth in model space due to the natural decay of kernel of gravity field with inverse distance square. The graph in Fig. 4.4 shows the sensitivity of the gravity kernel with a depth of the source body or model cell. As the graph revealed the sensitivity of the gravity kernel reduced exponentially with depth. Due to such reasons incorporating depth weighting function in inversion is become indispensable.

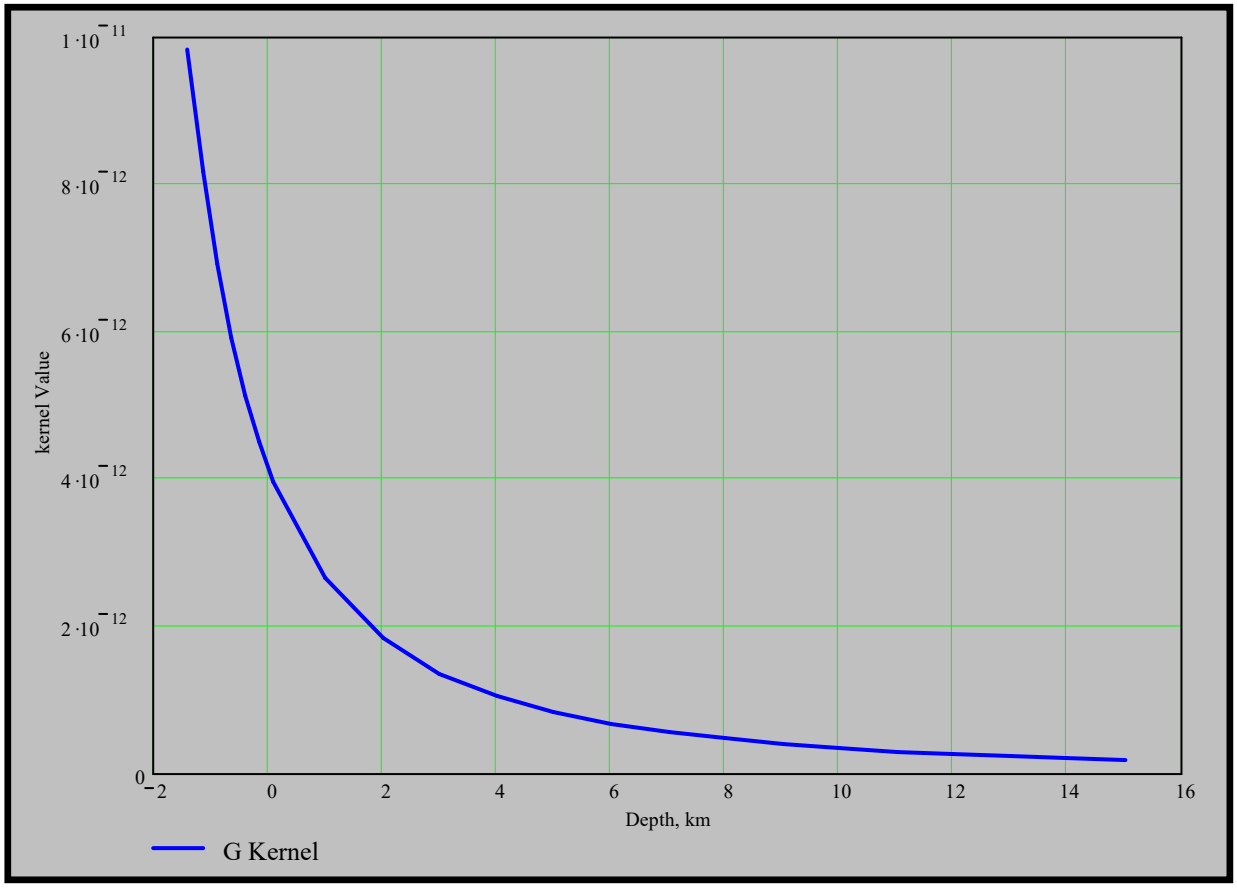

Figure 4.4 *Sensitivity of gravity kernel with depth*

After all necessary parameters, functions and constraints were prepared in an appropriate form for numerical computation; the inversion process was carried out based on the above-described

algorithm in the methodology section. Finally, the output model recovered from the inversion execution is demonstrated in the following successive paragraphs and figures.

From the inversion of the residual gravity anomaly of the study region, we observe four models; the first one is a horizontal slice of density contrast in the X-Y (E-N) plane that can help to reveal the major lateral density variation in the realm of the study region. The horizontal density contrast model illustrated in Fig. 4.5 is obtained from the execution of the 3D inversion of the Bouguer residual gravity anomaly.

The black rectangular region in the recovered density contrast image is the mineralization zone of southern green stone. From the solution of inversion, 76.8% of the pixels in the mineral zone are scored positive density contrast that is associated with the metallic mineral in the region. In addition percentage of the very high-density contrast category is 33% that reflects very high denser material. In contrast, the percentage of very low-density contrast under mineralization zone is 3.77% this indicates the target high density metallic mineralized region and the recovered result has made a correlation. Therefore this numerical evidence indicated inversion result has made a good agreement with the fact in the target area.

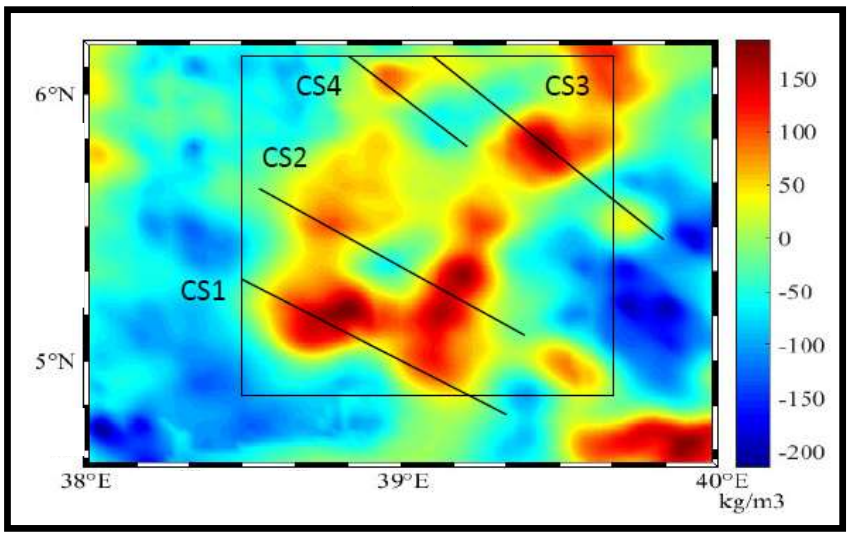

Figure 4.5 *Horizontal density contrast distribution*

In general terms high contrasting region associated with the massive concealed body is identified from the horizontal distribution of density contras

Table 4.1 Percentage and density contrast value of target region

	Percentage
Positive density contrast	76.8
Very high-density contrast	35
Very low-density contrast	3.77

Finally, an important output observed from the inversion procedure was taking the vertical cross-section or slice at a given plane in Fig 4.5 (from CS1 up to CS4). The vertical cross-section plane was identified from a horizontal slice of density contrast that has scored high positive density contrast, such area considered to be the place where massive bodies exist and used as a target region to explore underlying density distribution. Therefore to look deep in subsurface geology, taking a vertical slice is reasonable and good to examine vertical density variation in the region. The result observed from a vertical slice of subsurface geology at different four selected target zone is demonstrated as follow. The revealed orientation of line at Fig. 4.5 is selected for two general reasons; the first one is to correspond with the direction of flight line that helps for the sampled data as precise as possible. The second reason is to fit with borehole in the region as much as possible

Vertical slice 1 (CS1)

The inversion was performed for the CS1 profile that was selected from a horizontal slice, as described above this selected location are scored high positive density contrast that shown in Fig 4.5. Firstly for better resolving the model space discretization or model cells size (275 m x 150 m) was chosen to a smaller size than the model used in the 3D inversion. Then the inversion process and kernel formulation were carried out separately. To executing the inversion to this profile the residual anomaly was extracted from the total data along with the indicated profile CS1 at Fig 4.5. And the total number of model cells is 37290 (339 cells in horizontal x 110 cells in a vertical direction). All constraint applied in the previous inversion was used based on their respective size, location, and dimension of model parameters. To quantify the model parameters that were imaged from inversion results, as revealed in Fig 4.6 the perturbation of density anomaly that caused the observed anomalous gravity is illustrated clearly. This perturbation indicates the contrasting density relative to the host rock of the region. From the resulting model, we perceived three different characteristics of underlying density contrast: i) the first one is high-

density contrast region that is associated with high-density material intercalated within the host rock so that the region showed a significant positive anomaly than the surrounding. As we observed from the model there are two distinct anomalous regions are identified in the figure. The first one is indicated the higher positive anomaly concentrated around the axis of 5.18^0 N and the maximum extension in-depth direction attained at the axis then the magnitudes and depth extension gradually reduced away from the axis.

The density contrast observed in the region is within the range of -150 kg/m3 and 165 kg/m3. And the depth extension of maximum anomaly attained around 1309.464 m below the surface. The second target anomaly has less density contrast and size than the first one whether in a horizontal or vertical direction. The nature of the anomalous region is horizontally elongated from 4.9^0 to 5.0^0 N. And the nature of anomaly toward the depth is unlike the first one it attained the maximum extension around 1119 m from the surface. In general term, these anomalies are provided a major significant contribution for observed high residual gravity anomaly. And revealed two peek residual anomalies are happening because of such density contrast described above. ii) The second feature observed from the model is the low-density contrast region that is revealed in Fig 4.6 (illustrated at shallow depth represented by blue-colored left and right margin of the model). These anomalies are a direct cause for the valley that we observed in the profile of gravity anomaly (CS1). Such kind of features demonstrated in the model is associated with the low-density contrast relative to the background density trend of underlying subsurface geology. iii) The third features illustrated in the model are the low perturbed region; this illustrated the homogenous nature of contrast relative to the highest and lowest contrast. It did not mean the density distributions are homogenous rather to say the magnitude of density perturbation is less. Such features are broadly distributed entire portion of the model from shallow depth up to the deepest section of the model. The contrasts observed from the part are in the approximate range of +/- 20 kg/m ^{3}. The contribution of such features for the observed gravity anomaly profile is superimposed within the gravity anomalies caused by high perturbing density contrast.

In general, the depth extension of the high-density contrast material revealed here in the model has a similar pattern to the information obtained from the borehole log in the study area. As described under Table 4.2 below, from the total high-density contrast region 81.5% of pixels involved above 600 m depth, this reflects most of the causative bodies are at a shallow depth that

indicates the concealed high contrasting density is distributed in the described level of depth and the magnitude of contrast may relate with the concentration of ore.

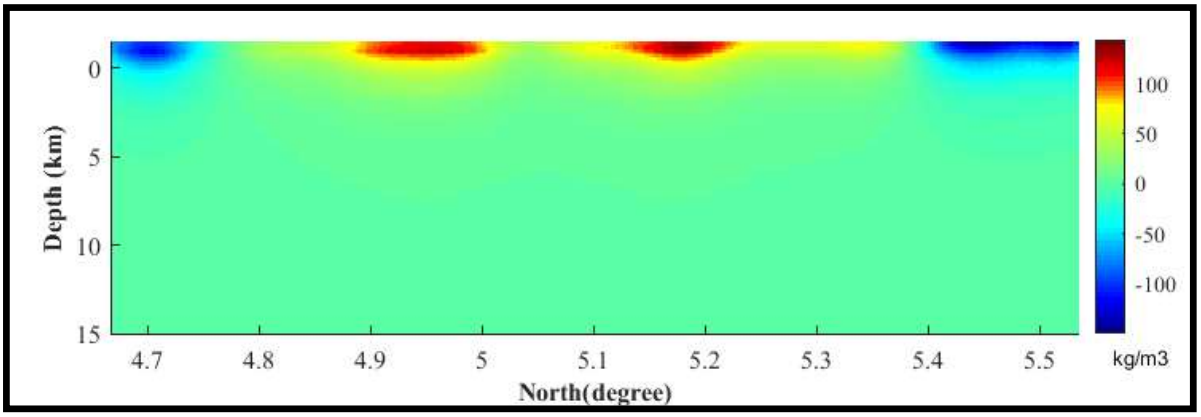

Figure 4.6 *Density contrast model at line CS1*

Vertical slice 2

The second vertical density contrast model obtained from the inversion of gravity anomaly of profile CS2 showed in Fig 4.5. The model discretization, data sampling, and other important input parameters applied in the inversion process were similar to the models described above. In general, the total numbers of model cells applied to run the inversion process for CS2 were 34239 (303 cells in horizontal X 113 cells in a vertical direction). The numbers of sampled data from total gravity anomaly along the profile were 303 point data. The unknown parameters obtained from the inversion of gravity anomaly are demonstrated below in Fig 4.7.

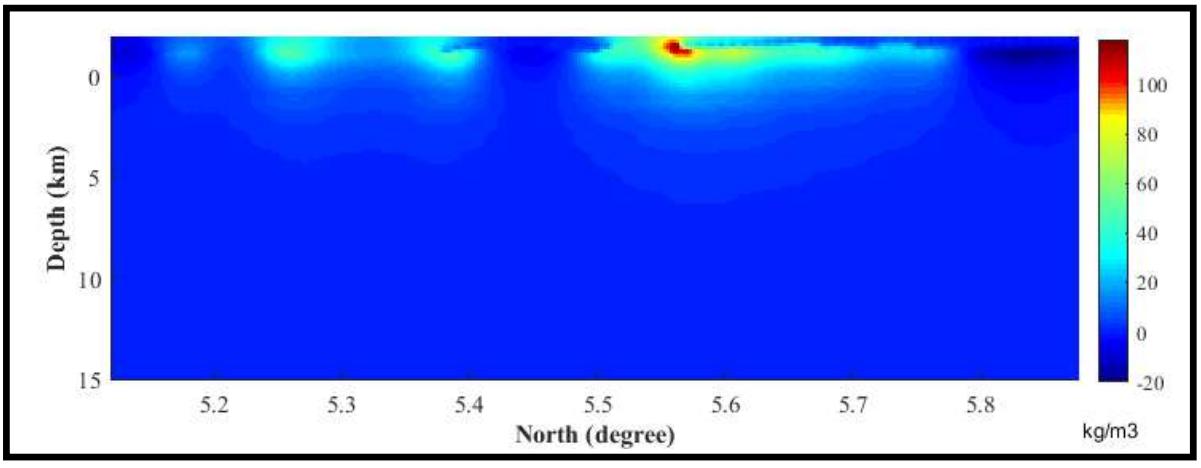

Figure 4.7 *Density contrast model at line CS2*

The density contrast model obtained from inversion revealed three important features: the first one is the blue region broadly distributed entire the model, this section of the model described

the less density contrast region i.e. most portion of the model scored within -20 kg/m ^{3} to 20 kg/m ^{3}.

The second feature revealed in the model is the higher density contrast region, as the model showed this feature is observed at shallow depth. The maximum extension of the body in the depth direction is 1089.866 m around the axis of 5.6^0 N and as the figure demonstrated the thickness of the anomalous density reduced in the north-south direction from the axis. In addition, moderate density contrast surrounding the higher one is sandwiched between low-density contrasts that extended horizontally. The general characteristics of the model illustrated in the figure are uniform regional contrast indicates the lateral uniformity of the underlying rock unit and on other hand; local contrasting area refers to high denser materials that are intercalated with the host rock. The bright blue spot we have observed in the model also indicates a relatively moderate density contrast distributed in the region.

As described under Table 4.2, from the total high-density contrast region 72% of pixels observed above 600 m depth, this reflects most the causative bodies are at shallow depth. This indicates the concealed high contrasting densities are distributed in the described level of depth and the magnitude of contrast may relate with the concentration of ore.

Table 4.2 For CS1 to CS4 high-density contrast maximum depth, average depth, standard deviation, and the percentage of high contrasting pixel above 600m depth

	Max. depth (m)	Average depth(m)	Depth <=600m (%)
CS1	1309.464	217.8736	81.5
CS2	1089.866	455.82	72
CS3	847.72	210.24	86.30
CS4	661.0338	262.6234	99.1

Vertical slice 3 (CS3)

The other vertical density contrast model obtained from the inversion of gravity anomaly of profile CS3 showed in Fig 4.5. The model discretization, data sampling, and other important input parameters applied in the inversion process were similar to the models described above. In general, the total number of model cells applied to run the inversion process for CS3 was 33787(299 cells in horizontal X 113 cells in a vertical direction). The numbers of sampled data from total gravity anomaly along the profile were 299 point data.

The unknown parameters observed from inversion were underlying density contrast of profile CS3 that is revealed in Fig 4.8. The nature of density contrast observed from the result has two important characteristics: the first one is a nearly uniform trend of density contrast values from shallow depth toward the deep direction. The second observed trend of density contrast has localized nature of density anomaly that revealed at a shallow depth of the model in a horizontal direction and in the vertical direction it extended from shallow depth to 847.72 m below the surface. The former trend of density contrast showed the background density of underlying subsurface geology. The latter demonstrated the local high-density materials assemblage in that locality of geological formation.

In general, the maximum value of density contrast observed was at the shallow depth of the model 127.5 m below the surface and gradually decrease from the center of the anomaly to outward as we can see from the figure the high-density contrasting region represented red to yellow color. On other hand, the minimum magnitude of density contrast observed was around 6^0 N and represented by blue color.

As described above under Table 4.2, from the total high-density contrast region 86.3% of pixels involved above 600 m depth, this reflects most of the causative bodies are at a shallow depth that indicates the concealed high contrasting density is distributed in the described level of depth and the magnitude of contrast may relate with the concentration of ore.

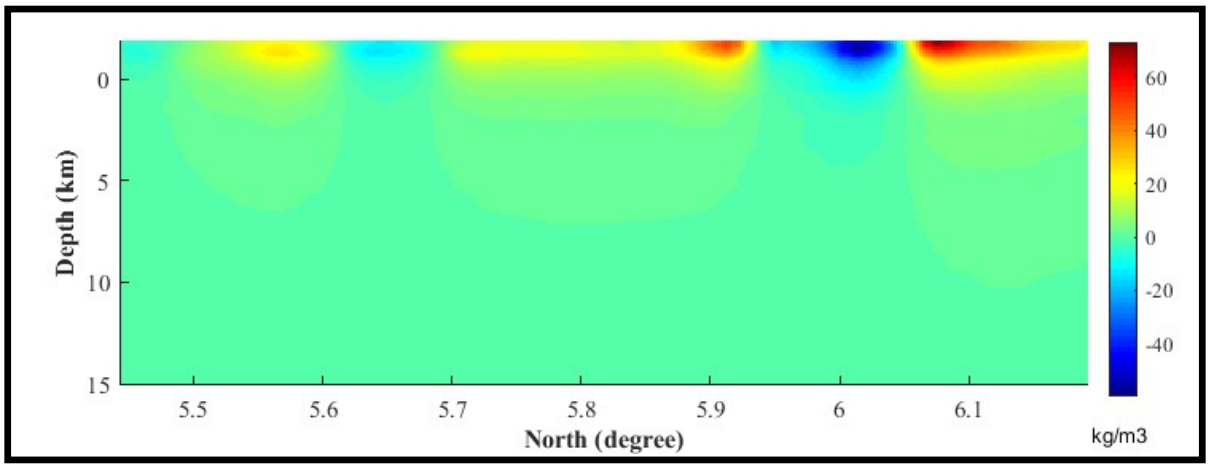

Figure 4.8 *Density contrast model vertical cross-section at line CS3*

Vertical slice 4(CS4)

The final vertical slice was the CS4 model that was observed from inversion of gravity anomaly data at the profile of CS4 shown in Fig 4.5. To execute the model discretization similar approach was applied with others, the model cell size is 275 m in a horizontal direction and 250 m in a vertical direction above mean sea level, and 1 km below mean sea level. 18908 model cells were prepared to carry out the inversion process. The residual gravity anomaly was extracted from total data along the profile CS4 illustrated in Fig 4.5. These and other necessary parameters that are described in the above section of the paper were prepared and organized in a form suitable to the inversion process.

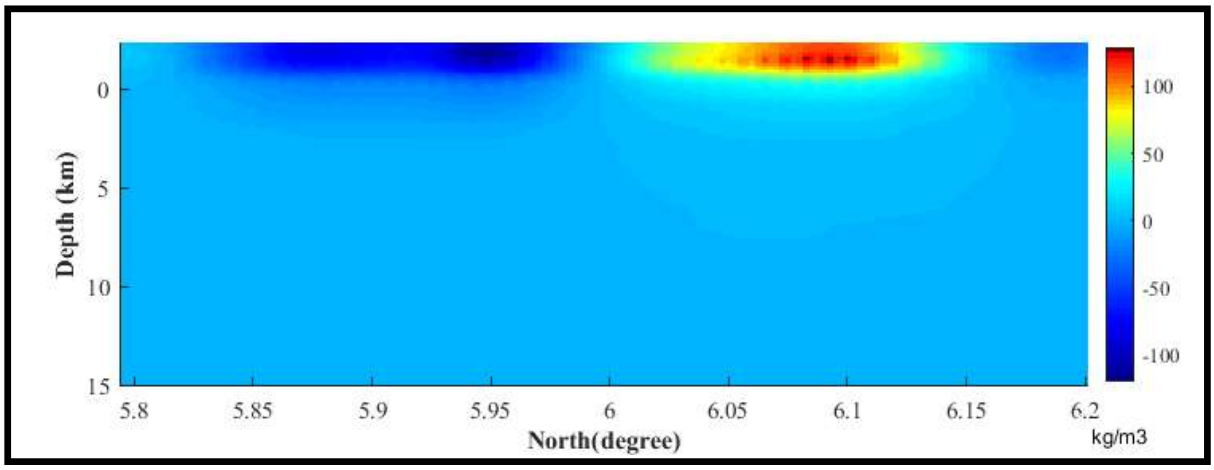

Figure 4.9 *Density contrast model at line CS 4*

The density contrast of the vertical slice recovered from the inversion is demonstrated below in Fig 4.9. The unknown density contrasts recovered from the inversion are illustrated in 3 main

characteristics. The first one represented by dark blue is associated with low-density contrast; the second one is represented from light blue to yellow color is related with moderate density contrast region that broadly distributed within the model and the range of density contrast in this domain is +/-50 kg/m ^{3}. The third one is illustrated at the top depth of the model and extended downward up to 661 m. This feature observed from the model was an anomalous density that hosted within the surrounding background density distribution. The higher anomalous density was recovered in the range of 6.05 to 6.12^0 N in a horizontal direction. The depth extent of higher anomalous density was observed from the top surface to 661 m toward the depth. Another significant anomalous density recovered in the model was a lower density anomaly located right near the higher anomaly. In general, the numerical density contrast values observed in the model are a maximum of 143 kg/m ^{3} at the higher anomalous region of the model at shallow depth from the surface then the contrast is gradually decrease away from the denser area. On other hand minimum, density contrast values observed in the model was -125 kg/m ^{3} around a shallow depth of the model that represented by dark blue color.

As described in Table 4.2 above, from the total high-density contrast region 99.1% of pixels involved above 600 m depth, this reflects most of the causative bodies are at a shallow depth that indicates the concealed high contrasting density are distributed in the described level of depth and the magnitude of contrast may relate with the concentration of ore.

4.5 Discussion

The basic parameters that were interested in, to recover density contrast by performing a 3D inversion of gravity anomaly have done and demonstrated in different angle as we have seen in the result section. The plane density contrast model obtained from inversion is demonstrated and identified the trend of high low-density contrast in the area of study. From the model, we perceived the spatial pattern where higher, lower and moderate density contrast recovered as well as other related parameters.

Based on the comparison of recovered results with the corresponding location of mineral potential map (Tadesse et al., 2003) 90.3% of high-density contrast regions have made a agreement with the location of mineral occurrences in the region. In addition, the major anomalous area identified in Fig. 4.5 demonstrated 76.8% of pixels in this region scored high-

density contrast. Based on such comparisons, the location of high-density contrast revealed under the result section (Fig. 4.5) is because of metallic mineral assemblage that intercalated throughout host rock of volcano-sedimentary sequences.

On other hands, the trend of high-density contrast at major anomalous areas revealed in Fig. 4.5 has made a good agreement with the geological condition that has been demonstrated in the previous studies. The mineralization trend in the region revealed in mineral potential map and previous studies (Mohammedyasin, 2017; Deksissa & Koeberl, 2004; Tadesse et al., 2003) , the occurrences of mineralization is highly associated with geologically fractured hydrothermal alteration of volcano-sedimentary rocks of Arabian-Nubian shield and the trends mineralization follows the fractures and N-S strike of the shear zone. Therefore N-S elongated high-density contrast trend revealed in the result (Fig. 4.5) is highly associated with high denser metallic minerals that follow the fracture and strike in the N-S trend.

On other hand, the vertical variability and continuity of metallic minerals in the region are determined from the geological cross-section or based on the information observed from the borehole. According to the information obtained from different borehole log synthesized in previous geological research of Getaneh (1994), metallic mineral concentration below the strike are revealed a variable concentration of ore mineral at different depth. Based on the diagram of various bore log the occurrence of metallic mineral in-depth direction are demonstrated from 22 m up to 590 m below the surface. In most pits, the concentration of metallic ore is strongly decreased at the bottom of the pit. As described under table 4.2 the percentage of high-density contrast at depth of fewer than 600 m demonstrated based on the respective percentage of high-density contrast is recovered within the expected depth range of mineral zonation in all vertical cross-section revealed through CS1 to CS4. Therefore based on the comparisons made between the mineralization conditions demonstrated in previous studies and current study indicated, the density contrast recovered from the inversion of gravity anomaly brought a consistent result in an aspect of the trend, location, and depth extension of density anomaly distribution particularly focused on high density contrasting condition and causative metallic resource.

Chapter Five

5. Conclusion and Recommendations

5.1 Conclusion

The 3D gravity inversion using Tikhonov regularization is performed for the target south green stone mineral zone. While solving the ill-posed problem various necessary informations were appropriately arranged to carry out the minimization process. Tikhonov cost function was used as an objective function that consists of three basic components: the first one was a residual norm that was used to control data misfit. The second component was model norms that helped to incorporate regularization parameters and model weight. The third one is the regularization parameter that helped to keep the balance between model norm and residual norms. The regularization parameter was chosen automatically using the L-curve criterion. After these, all appropriate functions were arranged. The next task was performing minimization of the Tikhonov cost function. Finally, after the minimization of the objective function was accomplished, at the end minimized function was rearranged in an appropriate fashion to carry out inversion using a conjugate gradient algorithm.

After the inversion was accomplished in such a way, the recovered result that was able to describe the model space was demonstrated well. The outputs obtained from the inversion were revealed in five images. The first section of the model showed the density contrast distribution in a horizontal plane that identified the high-density contrast region because of metallic mineral deposit at the southern green stone mineralization zone, this model showed 90.3% of correlation with the location of metallic mineral deposit. In addition, the model showed the trend of mineral occurrence this means as of the known information of geology the occurrence of mineral follows the trends of N-S strikes in the shear zone, those trends are similarly recovered in the horizontal slice density contrast model.

Another density contrast model observed from gravity inversion was a vertical slice at selected four vertical planes. These models clearly illustrated the vertical pattern of the ore body in an aspect of the depth resolution and lateral variability of high-density contrast associated with mineralization. The numerical correlations are demonstrated the degree of agreement in the depth direction and lateral continuity

Generally, the algorithm has been broadly been implemented for detecting various ore deposits in various research, here applied to detect metallic minerals especially gold minerals that has been abundantly distributed in the region of interest.

Therefore from the result and interpretation of this study the following points are concluded:

1) Gravity inversion is an effective tools for recover the signature of metallic mineral if appropriately implemented the algorithm 2) The parameters such as, delineating of a clear geometry, determination of size, depth location and the trends of mineralization that to be recovered from the inversion are highly depends on the amount of priori information to be incorporated in the inversion process and the resolution of gravity data. Therefore if we applied sufficient apriori information and enough resolution of data, it is possible to detect detailed information of the mineral deposits.

5.2 Recommendations

The investigation about subsurface geology is too complicated because the geological structure and mineral deposits are concealed underground. Such condition creates a difficult situation to interpret remotely sensed data. So the following recommendation provides some sort of direction to advance the interpretation process in future works.

During carrying out gravity inversion it is recommended to apply further geophysical and geological observed data as a priori knowledge that helps to improve the capacity of interpretation to a high level of certainty.

Utilizing well organized geological information database are required to establish for detailed investigation and successful interpretation of subsurface resource.

In addition, joint inversion algorithm is recommended to improve the resolution of the model in an aspect of enhancing the deep and detailed insight to ward subsurface geology.

A high gravity data resolution is recommended to exploration for finer scale mineral deposit

Bibliography

Alsadi HN, and Bahan EN. (2014) Introduction to gravity exploration method . Iraq: University of Sulaimani, Kurdistan Region.

Bevis M. (2017, June 21) igppweb. Retrieved Julay 05, 2020, from CRUST1.0 website: https://igppweb.ucsd.edu/~gabi/crust1.html

Cai H, Xiong B, and Zhu Y. (2018) 3D Modeling and inversion of gravity data in exploration Scale. INTECH, 19-37.

Calvettia D, Morigib S, Reichelc L, and Sgallarid F. (2000) Tikhonov regularization and the L-curve for large discrete ill-posed problem. Journal of computational and applied mathematics (ELSEVIER) , 423-446.

Chen Y, Zhao B, Huang J, and Zhang L. (2018) Application of BEMD in extraction of regional and local gravity anomalies reflecting geological structure associated with mineral resource. INTECH , 74-95.

Cornwell DG, Mackenzie GD, England RW, Maguire PKH, Asfaw LM, and Oluma B. (2006) Northern main Ethiopian Rift crustal structure from new high-precision gravity data. Geological Society of London, 307–321.

Deksissa DJ & Koeberl C. (2004) Geochemistry, alteration and genesis of gold mineralization in the Okote area, southern Ethiopia. Geochemistry journal, 38, 307-331.

Essa KS, and Elhussein E. (2018) Gravity data interpretation using different new algorithms: A comparative study. Intech Open, 4-17.

Essa KS and Munschy M. (2019) Mineral exploration from the point of view of geophysicists. Intech Open,1-10.

Ethiopian Institute of Geological survey (1989) Generalized geological and mineral oocurrcnccs of Ethiopia. Addis Ababa: Minster of mine and energy.

Getaneh W. (1994) Sulfide mineralization in the Lega dembi primary gold deposit, Sidamo southern Ethiopia. Addis Abeba university journa, 1-135.

Gupta PK. (2011) Linear inverse theory. Springer, 632-639.

Hansen PH. (2010) Discrete inverse problems insight and algorithm. Philadelphia: society for industrial and applied mathematics Philadelphia.

Jones F. (2007) Gravity survey. UBC Earth and Ocean Sciences, 1-18.

Kearey P, Brooks M, and Hill I. (2002). An introduction to geophysical exploration. Hong Kong: TJ International, Padstow, Cornwall.

Lane R. (2004) Airborne gravity 2004 – Abstracts from the ASEG-PESAAirborne gravity 2004 Workshop: . Australia: Geoscience of Australia.

Liang Q, Chen C, and Li Y.(2014) 3-D inversion of gravity data in spherical coordinates with application to the GRAIL data. J. Geophys. Res.Planets. 119, 1359-1373.

Li Y, and Oldenburg DW. (1998) 3-D inversion of gravity data. GEOPHYSICS, 109–119.

Mahatsente R, Jentzsch G, and Jahr T . (1999) Crustal structure of the main Ethiopian rift from gravity data: 3-dimensional modeling. Tectonophysics (ELSEVIER), 363–382.

Mandal A, Mohanty WK, Sharma SP, Biswas A, Sen J and Bhatt AK (2019) Geophysical signatures of uranium mineralization and its subsurface validation at Beldih, Purulia District, West Bengal, India: a case study. EAGE, 713–726.

Mohammedyasin MS. (2017) Geology, Geochemistry and Geochronology of the Kenticha rare metal granite pegmatite, Adola belt, southern Ethiopia: A review. International Journal of Geosciences, 8, 46-64.

Olesen A , and Forsberg R. (2007) The Ethiopia 2006 airborne gravity survey. Data acquisition and processing report. Addis Ababa: Danish National Space Center(DNSC).

Richter M. (2016) Inverse problems basics theory and application in geophysics.Neubiberg, Germany: Birkhäuser.

Sambridge M, and Gallagher K. (2011) Inverse theory: Monte Carlo method. Canberra seismology and mathematical geophysics, research school of Earth sciences, The Australian National University, Canberra, Australia.

Sandham WA, and Hamilton DJ. (2011) Inverse theory: Artificial Neural Networs. Edinburgh: springer.

Seeber G. (2003) Satellite Geodesy. Berlin: Walter de Gruyter.

Tadesse S, Milesi JP, and Deschamps Y . (2003) Geology and mjneral potential of Ethiopia: a note on geology and mineral map of Ethiopia. Journal of African Earlh Scicnces (ELSEVIRR) , 273 -113.

Tefera M, Chernet T, and Haro W. (1996) Explanation of the geological map of Ethiopia (2nd eddition). Addis Abeba: Ethiopian institute of geological survey.

Tiber C, Ebinger C, Ballu V, Stuart G and Oluma B. (2005) Inverse model of gravity data from Red Sea-Aden-East African Rift Triple. Geophysic J.int., 775-787.

Valenta J. (2015) Introduction to Geophysics. Czech republic: Czech republic development cooperation.

Vatankhah S, Ardestaniy VE, Niriz SS, Renautx RA, and Kabirzadeh H. (2019) A MATLAB Package for 3D inversion of gravity data using graph theory. IGUG , 1-19.

Appendix

As described under method section the Tikhonov cost or objective function has been used to minimize the problem. The minimization process was carried out by differentiation of the objective function as follow. After minimized the function at the end rearrange the matrix in order to get positive definite matrix which is called sensitivity matrix.

Tikhonov cost function

$\varphi=\varphi d + \lambda\varphi m \quad => \ ||wd(g-Gp)||^2 + \lambda||wm(p-p_0)||^2$

$[wd(g-Gp)]^2= \ [wd(g-Gp)]^T \ [wd(g-Gp)],$

$[wm(p-p_0)]^2= \ [wm(p-p_0)]^T \ [wm(p-p_0)],$

$\varphi= \ [wd(g-Gp)]^T \ [wd(g-Gp)] \ + \lambda \ [wm(p-p_0)]^T \ [wm(p-p_0)]$

$\varphi= \ g^T W_d{}^T W_D g \ - \ 2p^T G \ {}^T W_d{}^T W_d g \ + \ p^T G^T W_d{}^T w_d G p \ + \ \lambda(p^T W_m{}^T W_m{}^T p \ - \ 2p^T W_m{}^T W_m p_0 \ + \ p_0{}^T W_m{}^T W_m p_0)$

$\frac{d\varphi}{dp} = \ \frac{d\varphi_d}{dp} + \ \lambda \frac{d\varphi_m}{dp} = 0 \ ,$ $\qquad \frac{d\varphi_d}{dp} \ = -2G^T \ W_d{}^T W_d g + 2G^T W_d{}^T w_d G p$

$\frac{d\varphi_m}{dp} \ = 2W_m{}^T W_m{}^T p - 2W_m{}^T W_m p_0$

$\frac{d\varphi}{dp} = \ -2G^T \ W_d{}^T W_d g + 2G^T W_d{}^T w_d G p + \ 2\lambda W_m{}^T W_m{}^T p - 2\lambda W_m{}^T W_m p_0 = 0$

$-2G^T \ W_d{}^T W_d g + 2G^T W_d{}^T w_d G p + \ 2\lambda W_m{}^T W_m{}^T p - 2\lambda W_m{}^T W_m p_0 = 0$

$2G^T W_d{}^T w_d G p + \ 2\lambda W_m{}^T W_m{}^T p = 2G^T \ W_d{}^T W_d g + 2\lambda W_m{}^T W_m p_0$

$2p(G^T W_d{}^T w_d G + \ \lambda W_m{}^T W_m{}^T) = 2(G^T \ W_d{}^T W_d g + \lambda W_m{}^T W_m p_0)$

$(G^T W_d{}^T w_d G + \lambda \ W_m{}^T W_m{}^T)p = G^T \ W_d{}^T W_d g + \lambda \ W_m{}^T W_m p_0$

Then

$B= G^T W_d{}^T w_d G + \ \lambda W_m{}^T W_m{}^T$

$l= G^T \ W_d{}^T W_d g + \lambda W_m{}^T W_m p_0$

$B\triangle p \ = \ l$ where B is sensitivity matrix. l is known right hand side

B. Free air gravity anomaly map of study region